The color selectivity of neurons in posterior inferior temporal cortex of macaque monkey

The Graduate University for Advanced Studies
National Institute for Physiological Sciences

Masaharu Yasuda

Table of Contents

SUMMARY AND CONCLUSIONS

Inferior temporal (IT) cortex of the monkey is the final stage of the ventral stream that is concerned with the processing of color and shape information. Lesion studies indicated that IT cortex plays an important role in color perception. Previous recording studies showed that there were many color selective neurons in the anterior two-thirds of IT cortex (area TE). As for the posterior IT (PIT) cortex, although some imaging studies reported that this area is activated by color stimuli, no neural recording experiments have been conducted to systematically study color selectivity of PIT neurons. In the present study, we recorded neuron activities from PIT cortex and examined color and shape selectivity using a set of color stimuli that systematically distributed in the color space and a set of geometrical patterns. Neurons were recorded from three hemisphere of two macaque monkeys while each animal performed a visual fixation task. Recording chambers were placed to cover the lateral surface of the PIT cortex anterior to the inferior occipital sulcus.

We recorded 727 single and multiple neurons from PIT of two monkeys, and examined the color selectivity, shape selectivity and extent of the receptive field (RF) of each neuron, and studied how these response properties distributed in PIT cortex. We found that many color-selective neurons distributed throughout the PIT cortex examined. However, the color selective properties were not homogeneous across the PIT cortex. We found that neurons in the ventral part of PIT cortex tended to have sharper color tuning than those in the dorsal part of PIT cortex. We also found that many PIT neurons exhibit shape selectivity, and that color selective neurons with and without shape selectivity were intermingled in either the dorsal and ventral region of PIT cortex. This suggests that the processing of color information and shape information takes place in close relationship in PIT.

We quantitatively tested the color and/or shape selectivity in 197 single neurons. In these neurons, we quantified the selectivity to color and shape stimuli of each neuron using two indices. First, selectivity index was calculated for each neuron to quantify how well a cell discriminated the most-preferred stimulus from the least-preferred stimulus in each set of stimuli. The value of selectivity index and the statistical significance of the variation in the responses to the stimulus sets were used to classify a neuron as selective or not. Secondly, we calculated sparseness index to quantify the sharpness of stimulus selectivity. This index indicates the degree to which responses evenly distributed across the set of stimuli. We mapped the distribution of these indices across the PIT cortex, and found that color selective neurons with sharp color tuning (color sparseness index < 0.7) were concentrated in the ventral part of PIT cortex examined and we named this region as PIT

color area (PITC). In PITC, each neuron had sharp color tuning and represented only a restricted area of the color space, but the population of such sharply color-tuned neurons in PITC as a whole represented the entire color space. Neurons located out of PITC also had color selectivity but they tended to have broader color tuning than those in PITC. With regard to the strength and sharpness of shape selectivity, there was no clear difference between neurons located in and out of PITC.

We mapped the RFs in PIT and found that there was crude retinotopic organization in PITC. Neurons in the dorsal part of PITC had RFs containing the foveal center. In the ventral part, the eccentricity of RFs increased and the RFs in the anterior and posterior part represented the lower and upper visual field, respectively. This retinotopy corresponded well to what Boussaoud et al. (1991) previously reported in PIT. One important difference between their previous result and our present result is that, although these authors reported that the retinotopic map covered the entire region of the lateral surface of PIT cortex ventral to STS, we found that clear retinotopic organization was restricted within a part of PIT and this area corresponded to the region where neurons having sharp color selectivity were concentrated, namely PITC. Moreover, the position of the retinotopic map differed between individual hemispheres, and the positional shift seemed to be in coincident with the variation of the position of PMTS. The present results strongly suggest that there is a circumscribed region in and around PMTS that has crude retinotopic organization and that is involved in the processing of color information.

As the luminance contrast is an important factor influencing the perceived color, we used two color stimulus sets at two different luminance contrasts; one is darker and the other is brighter than the background. Many PITC neurons changed their responses to color stimuli depending on their luminance contrast. When we considered the color representation with the activities of the entire population of neurons, we found that the responses to red and blue were stable across two luminance contrasts while the responses to un-saturated colors such as white, gray, and black were variable with the change in luminance contrast. This seems consistent with the fact that the perceived color of un-saturated colors significantly change depending on the luminance contrast whereas that of blue and red do not change by the change in the luminance contrast. These results suggest that activities of color selective neurons in PIT cortex is strongly related to color perception.

INTRODUCTION

In the monkey visual cortex, color information is transmitted along the ventral visual pathway through areas V2 (Hubel and Livingstone 1987) and V4 (Zeki 1973; Schein and Desimone 1990), then reaches to the inferior temporal (IT) cortex (Tanaka et al. 1991; Komatsu et al. 1992). Lesion studies have shown that damage of IT cortex severely disrupts color discrimination (Horel 1994; Heywood and Cowey 1995; Buckley et al. 1997; Huxlin et al. 2000; Cowey et al. 2001), suggesting that IT cortex plays an important role in color vision in monkeys. To understand how color information is processed in IT cortex, it is important to know how color information distributes or localizes in IT cortex. However, little is known about this problem.

IT cortex is divided into two parts (Bonin and Balley 1947; Iwai and Mishkin 1969) ; area TE occupies the anterior two-thirds and area TEO occupies the posterior one-third. Area TE includes the anterior and central IT cortex, and area TEO corresponds to the posterior IT (PIT) cortex (Van Essen et al. 1990). In the present study, we will use the term PIT instead of TEO to avoid confusion because TEO is also used in a more specific manner to indicate a retinotopically organized area (see below). Neural recording experiments have shown that many color selective neurons exist in area TE (Komatsu et al. 1992; Komatsu and Ideura 1993) but there has been no systematic study investigating the color selective properties in PIT cortex. A positron-emission-tomography (PET) imaging study (Takechi et al. 1997) during a color discrimination task and a 2-deoxy-glucose (2DG) imaging study (Tootell et al. 2004) have shown that color stimuli evoked strong activation in PIT. These results suggest that PIT is involved in the processing of color information. In the present study, we systematically analyzed the color selectivity of neurons in PIT using stimuli based on color space, and examined how color selective neurons distribute in this area. It has been demonstrated that lesion of PIT severely disrupts pattern discrimination (Iwai and Mishkin 1969), and that many neurons in this area exhibit shape selectivity (Tanaka et al. 1997; Brincat and Connor 2004). Therefore, we also examined shape selectivity of the same group of neurons using a set of geometrical shapes.

An important problem in this study is how to define the extent of PIT. PIT cannot be clearly segregated cytoarchitectonically (Bonin and Balley 1947) or mieloarchitectonically (Boussaoud et al. 1991) from the surrounding regions sucha as areas TE and V4. Lesion studies have commonly employed sulcal landmarks to delineate the boundary of PIT (Heywood and Cowey 1995; De weed et al. 1999; Huxlin et al. 2000; Cowey et al. 2001); its posterior border is at or just anterior to the anterior tip of the inferior occipital sulcus (IOS), and the anterior border is at the anterior end of the posterior middle temporal sulcus (PMTS).

In the present study, we determined the extent of the recording sites based on these sulcul landmarks. On the other hand, Boussaoud and colleagues conducted a detailed mapping of the receptive fields (RFs) from in and around PIT, and demonstrated that there exists crude retinotopy of the contralateral visual hemi-field on the lateral surface of the inferior temporal gyrus between the anterior tip of IOS and the anterior end of PMTS (Boussaoud et al. 1991); central visual field is represented dorsally and, in more ventral area, anterior region represents the lower visual field and the posterior region represents the upper visual field. These authors called this retinotopically organized area as TEO. Thus, in the present study, we also conducted RF mapping, and attempted to examine how such retinotopic organization is related to the color selective properites of neurons.

We found that many color selective neurons exist in PIT. However, there was difference in the degree and sharpness of color selectivity between the dorsal and ventral parts within PIT; neurons with sharp color selectivity were concentrated in the ventral part and we found this ventral region had crude retinotopy that was consistent with a previous report. In both the dorsal and the ventral parts, many neurons had shape selectivity. These results suggest that PIT is strongly related to the processing of color as well as shape information.

METHODS

Behavioral task

Two awake macaque monkeys (*Macaca fuscata*) were used for the experiments. All procedures for animal care and experimentation were in accordance with the National Institutes of Health Guide for the Care and Use of Laboratory Animals and were approved by the animal experiment committee of the Okazaki National Researdh Institutes.

During the experiment, monkeys were seated on a primate chair and faced a CRT monitor 56 cm in front of the monkey. The width and height of the monitor was +/- 20 degrees and +/- 15 degrees. The monkeys were trained to fixate a small white dot (fixation spot, 50 cd/m^2, 0.1 degrees) presented at the center of the monitor. A trial started when the fixation spot turned on. When the monkey maintained fixation for 500 ms, a visual stimulus was presented at a certain position of the monitor for 500 ms. When the monkey maintained fixation for 760 ms after stimulus offset, the fixation spot was disappeared and a drop of sports drink was given to the monkey as a reward. When the visual stimulus was presented at the foveal center, the fixation spot was turned off from 350 ms before visual stimulus onset until 260 ms after stimulus offset. The monkey's gaze was monitored by the scleral search-coil technique (Robinson 1963). The monkeys were required to maintain fixation within an eye window (+/- 1.5 deg for monkey KM and +/- 0.75 deg for monkey MA) throughout the trial. When the monkey's gaze was deviated from the eye window, the trial was aborted.

Surgey and recording

Under sodium pentobarbital anesthesia, sterile surgery was conducted to attach a head holder and a recording chamber on the skull by dental cement and implanted bolts. The head holder was used to connect the monkey's head to the primate chair. A search coil was placed under the conjunctiva of one eye and was connected to a plug on top of the skull. The recording chamber was placed laterally on the skull to cover the posterior part of the inferior temporal cortex. Before surgery, the position of the superior temporal sulcus (STS), the inferior occipital sulcus (IOS) and the posterior middle temporal sulcus (PMTS) were identified by MRI scans. A recording chamber was placed to cover the region anterior to IOS and the region dorsal and ventral to PMTS. Also, at the end of most recording sessions, we confirmed the location of electrode by taking X-ray images (left hemisphere in monkey MA).

Vanish-coated tungsten microelectrodes (Frederick Haer) or elgiloy electrodes were penetrated through the dura using a hydraulic microdrive (Narishige) to record neuron activities extracellularly. To precisely locate the electrodes, they were advanced through a stainless guidetube that was holded by a plastic grid with holes (Crist et al. 1988). The distance between each hole was 1mm and by using two types of grids that were shifted 0.5 mm vertically and horizontally each other, the minimum interval between holes was 0.7 mm.

Neural signals were amplified, sampled at 25 kHz and stored in the computer for off-line analysis. Behavioral events were recorded at 1 kHz. Neural signals were also discriminated on the basis of spike amplitude and converted to pulses and displayed on line as rasters and peri-stimulus-time-histograms (PSTHs) to inspect the visual response. Neural signals and isolated pulses were fed to a speaker for audio monitoring. At the end of several electrode penetrations, markings were made by passing tiny currents through the tip of the electrodes.

At the end of the experiments, monkey KM was deeply anesthetized with sodium pentobarbital and perfused through the heart with saline followed by 4% paraformaldehyde plus 2% ferrocyanide. The brain was then removed from the skull, sectioned in the frontal plane, and stained with cresyl violet. The sites of electrode markings were identified on the histological sections under microscopic examination.

Visual stimuli and Test of selectivity

Visual stimuli were generated using a graphic board (VSG2/3, Cambridge Research) in a computer and displayed on a CRT monitor (Sony GDM-F500R; 800 × 600 pixels, 40 deg horizontally x 30 deg vertically; 142 frames/s). Figure 1 shows a standard set of colors and shapes we used in the present experiment. Stimulus colors were defined on the basis of the CIE 1931 xy chromaticity diagram (Fig. 1a). A triangular region on the chromaticity diagram indicates the range of colors that can be displayed by the CRT monitor used. To test color selectivity of neurons, we used two sets of color stimuli. Each set consisted of 15 colors whose chromaticity coordinates were evenly distributed on the CIE xy chromaticity diagram (1-15 in Fig. 1a). In one set, each stimulus had the same luminance (20 cd/m^2) except for the blue color (#15, 11 cd/m^2) that were higher than the luminance of the gray background (x = 0.3127, y = 0.3290, 10 cd/m^2). In another set, the luminance of stimuli (5 cd/m^2) was lower than the background. Occasionally, we used a third set of colors that were brighter than the background and all colors had the same luminance (11 cd/m^2). In addition to these 15 colors, neutral gray stimuli (x = 0.3127, y = 0.3290) with the same luminance (either 20 cd/m^2 or 5 cd/m^2) were tested. To coarsely test the color selectivity,

we used another set of 16 colors that consisted of 7 colors (1, 3, 5, 10, 12, 15 and W in Fig. 1a) at two luminance levels (20 cd/m^2 and 5 cd/m^2) together with white and black stimuli. When we tested color selectivity, the shape of the stimuli were fixed and chosen from 11 geometrical shapes (Fig. 1b; square, diamond, circle, star, cross, oblique cross, triangle, vertical bar, oblique bar in clockwise direction, horizontal bar and oblique bar in counterclockwise direction). Each of these shape stimuli was painted homogeneously with a single color. To test shape selectivity of neurons, we usually used these eleven shapes, but in some experiments, 4 bar stimuli were not tested. The chromaticity coordinates and the luminance of the stimuli were measured by using a spectrophtometer (PhotoResearch PR-650).

For each neuron, we determined the optimum stimulus color, shape, position and size by using the visual stimulus sets described above. To test the color (shape) selectivity quantitatively, shape (color) of the stimuli were fixed to the optimum parameter of that neuron. In each trial, a stimulus was chosen randomly from the stimulus set and trials were repeated until each stimulus was presented six times. RF mapping was conducted by presenting preferred stimulus in various positions in the visual field. All visual stimuli used were stationary flash stimuli. Neural recordings were separated at least 100 um in distance in each electrode penetration.

Data analysis

For off-line analysis of neural data, we first isolated spikes by using template matching algorithm in temporal resolution of 1 ms. We then computed the average firing rate of the isolated spikes during stimulus presentation period (50-550 ms after stimulus onset). Then we subtracted from this the average firing rate before stimulus presentation (300-0 ms before stimulus onset, baseline activity). We used this value as the measure of the neuronal response to visual stimulus. Only those neurons whose responses to the optimal color was larger than 10 spike/s and whose discharge rates during stimulus presentation were significantly different from baseline activity (Student's t test, $P<0.05$) were included in the sample for analysis. To quantify the strength of color and shape selectivity of each neuron, a selectivity index was calculated as 1 – (minimum response)/(maximum response). We also evaluated whether the variation in the responses to stimuli within a set of test stimuli was significant by one-way analysis of variance (ANOVA). When the selectivity index was larger than 0.6 (maximum response was more than 2.5 times the minimum response) and response variation was significant (ANOVA, $P<0.05$), responses of a neuron was regarded as stimulus selective. To quantify the sharpness of stimulus

selectivity, we calculated sparseness index (Rolls and Tovee, 1995), which was defined as

$$\text{sparsness index} = \left(\sum_{i=1,n} r_i / n \right)^2 / \sum_{i=1,n} (r_i^2 / n)$$

where r_i is the firing rate to the i th stimulus in the set of n stimuli. If r_i was negative value, it was replaced to zero. This index indicates the degree to which responses evenly distributed across the set of stimuli. When all stimuli evoked the same response amplitude, the sparseness index had a maximal value of 1. When the stimulus selectivity became sharper, this index becomes smaller. If only one stimulus among the set evoked the response, the index value became minimum and was equal to 1/n. When we tested the color selectivity at two luminance levels, we determined these indices on the color selectivity based on the responses obtained at the luminance in which the largest response was evoked.

We mapped the receptive fields (RF) of each neuron on-line by presenting the preferred stimulus at various positions on the display, and determined the horizontal and vertical extent of the RF. The RF was approximated by rectangle whose contours overlapped with the edges of the RF. When one edge of the rectangle exceeded the extent of the CRT monitor, the eccentricity of the edge of the monitor (+/- 15 degrees vertically and +/- 20 degrees horizontally) was assigned as that of the RF. Center of the RF was determined as the mid-point of either the horizontal or vertical extents of the RF. Eccentricity of the RF was determined as the distance between foveal center and the RF center. When more than two sides of the rectangle were over the extent of the monitor, RF was classified as having the eccentricity of the center larger than 8 deg. To investigate the distribution of RF across the recorded area, we first distinguished two types of the RFs depending on whether we could determine the entire border of the RF. If the entire border was determined, we defined the RF center as the average of the vertical and horizontal extents of the RF. For these neurons, the RF in which the eccentricity of its center was less than 2.5 degrees was classified into “fovea”. Of the remaining neurons whose entire RF border was determined, if the RF center was in the upper (lower) visual field and was located within +/- 60 degrees from the vertical meridian, the RF was classified as “upper (lower) visual field”. In other cases, RF was classified into “horizontal meridian”. When the entire RF border was not determined, we classified the RF into the same four groups as above according to the mean position of the RF extent that could be determined.

RESULTS

Recording sites in PIT

We conducted recordings from PIT in three hemispheres of two monkeys. We recorded 289 single and multiple neurons from the left hemisphere of monkey KM and 246 and 192 neurons from the left and right hemispheres of monkey MA, respectively. We examined the color selectivity, shape selectivity and extent of the receptive field of each neuron, and studied the spatial distribution of these response properties in PIT. Of these neurons, we quantitatively tested both color and shape selectivities in 205 single neurons (KM: 67, MA-L; 18, MA-R;76). We found that there existed many neurons sharply tuned for color in a region around PMTS and that this region had crude retinotopy. Figure 2B and C show MRI images of the recorded hemispheres. As can be seen in this figure, PMTS was located more ventrally in both hemispheres of monkey MA (Fig. 2C) than that in the left hemisphere of monkey KM (Fig. 2B). Because of this, it was easier to access to the cortex near PMTS in monkey KM than in either hemisphere of monkey MA. As we will describe below, sharply color-tuned neurons were concentrated in a region around PMTS, and we were able to conduct more extensive mapping from this region in the left hemisphere of monkey KM. Thus, in the following, we will first present the results of mapping from this hemisphere in detail, and then describe the results obtained from both hemispheres of money MA.

Distribution of color/shape selectivity in PIT of monkey KM

Figure 3A shows the recording sites of KM, and a red square indicates the position of the recording chamber. The recorded sites covered the region both dorsal and ventral to PMTS. The rostral edge of the Inferior occipital sulcus (IOS) was located at the posterior end of the chamber. So we can think that most of the recorded sites belonged to PIT (see Fig. 2A). Figure 3B shows an example of the marking at the tip of an elgiloy electrode, and the penetration site of this electrode is indicated by arrows in Fig. 3A and C. We found that considerable number of neurons responded differently to colors in the stimulus set (color-selective neuron), and they widely distributed in the recorded sites. Of the 289 single and multiple neurons recorded from KM, we determined both color selectivity and shape selectivity in 144 neurons. For these neurons, the distribution of stimulus selectivity is shown in Fig. 3C in which stimulus selectivity of each neuron is indicated by symbols and plotted at the coordinate of penetration sites within the grid where the responses were recorded. Red symbols represent color selective neurons, and it can be clearly seen that

many neurons had color selectivity (130/144: 90.3%). Some of these neurons (88/130: 67.7%) had shape selectivity as well (red stars) and others (42/130: 32.3%) had no shape selectivity (red circles). The spatial distributions of these two types of neurons were intermingled.

Color selective responses in PIT

Figure 4 shows the responses of three example color selective neurons recorded from PIT of KM. Responses to the standard sets of color and shape stimuli are shown by rasters and histgrams on the left side. To the right on the top row, response magnitudes to color stimuli are represented by diameters of circles and are plotted at positions that correspond to their chromaticity coordinates. On the bottom row, responses to shape stimuli are plotted as a line graph. In all three neurons, clear differences in response magnitude were observed with different colors. Color selectivity indices of these neurons were larger than 0.6 and they showed statistically significant variation in response across different colors (ANOVA, $P < 0.05$). The neuron whose responses are indicated in Fig. 4A showed strong responses to red colors and that in Fig. 4B responded selectively to blue and cyan colors. The neuron in Fig. 4C showed both on- and off-responses; it showed selective on-response when green colors were presented, and it also showed selective off-response after purple colors were turned off. Interestingly, the color evoking on-response and that evoking off-response are complementary colors each other. We found such combination of on- and off-responses by complementary colors in 8 PIT neurons. As for responses to shape stimuli, the neurons in Fig. 4A and C did not exhibit shape selectivity (selectivity index is 0.42 in A and 0.32 in B), while the neuron in Fig. 4B showed clear shape selectivity and most strongly responded to cross shape (selectivity index = 1.01).

The preferred color, strength and sharpness of color selectivity differed from cell to cell. Figure 5 shows the responses of eight examples of color-selective neurons. Of these, six example neurons (from A to F) had sharp color tuning and responses were evoked only by specific range of hues; preferred hue was cyan (A), blue (B), green (C), yellow (D), red-purple (E) and achromatic colors around gray (F), respectively. We can conceive that the entire color space examined was represented by responses of these sharply color-tuned neurons as a whole. The remaining two neurons in Fig. 5G and H had broader color tuning that covered a wide region of the color space.

Concentration of sharply-tuned color selective neurons in PIT

We found that neurons having sharp color tuning as was the case for neurons indicated in Fig. 5A-F tended to be concentrated in postero-ventral two-thirds of our recorded sites. This can be seen from the distribution of sparseness index that indicates the sharpness of color tuning (Fig. 6). In this figure, the sparseness index of single neurons in which color selectivity was quantitatively examined is indicated at the coordinates of the grid where each neuron was recorded. The example neurons shown in Fig. 5 had sparseness index of 0.23, 0.41, 0.55, 0.61, 0.61, 0.65, 0.78 and 0.97 from A to H, respectively, and are indicated by alphabets. All the six neurons (A-F) that showed sharp color tuning have the sparseness index values less than 0.7, whereas the two neurons (G and H) with broad color tuning had the values larger than 0.7. So, in order to clarify the localization of sharply color-tuned neurons, we marked the values less than 0.7 with thick line in Fig. 6. It can be clearly seen that many neurons in the postero-ventral two-thirds of the recorded sites had index values less than 0.7 whereas only a small number of neurons had index values less than 0.7 in the remaining more dorsal area. This tendency did not change even when different values of the sparseness index such as 0.5 or 0.6 were used as the criterion. This result indicates that although color-selective neurons widely distributed in PIT, PIT is unlikely a homogeneous area and should be divided into at least two segments of the dorsal and ventral sub-regions based on the sharpness of color tuning. Neurons having sharp color tuning mainly existed in the ventral sub-region and this suggests a possibility that this region is more strongly related to the processing of color information. Therefore, in the following, we will distinguish the dorsal and the ventral regions and tentatively call the ventral sub-region as PIT color area (PITC).

Quantitative analysis of color and shape selectivities of PIT neurons

To systematically examine the color selectivity and shape selectivity of neurons in two sub-regions of PIT as described above, we calculated two indices (selectivity index and sparseness index) of each single neuron and the distribution of the indices is shown for neurons in PITC (Fig. 7A, B, E, F) and for those recorded out of PITC (Fig. 7C,D,G,H). Filled bars indicate neurons that were classified as color-selective (A-D) or shape selective (E-H). As for color selectivity, most PITC neurons (44/55, 80%) had the selectivity index value larger than 1 and many (43/55, 78.2%) had sparseness index value less than 0.7. This indicates that many PITC neurons showed strong and sharp color selectivity. On the other hand, neurons recorded out of PITC tended to have smaller value of the selectivity index (<0.6, n = 5, 22.7%) than those of PITC neurons and most of them had sparseness index value larger than 0.7 (figure 8D, <= 0.7: n = 4, > 0.7: n = 19). These results indicate

that neurons out of PITC have weaker and broader color selectivity than PITC neurons.

As for shape selectivity, we found no clear difference between the neurons recorded from PITC and those recorded out of PITC. Shape selectivity index widely distributed from large to small values both in and out of PITC (Fig. 8E, selective: n = 31, non-selective: n = 18, figure 8G, selective: n = 22, non-selective: n = 10). The distribution of sparseness index in both areas are biased toward large values. This indicates that neurons in both sub-regions tended to have broad shape tuning.

As shown above, many PITC neurons had sharp color tuning and each of them represented a restricted area of the color space. To examine whether the population of such sharply color-tuned neurons in PITC represent the entire color space or not, we averaged the responses of PITC neurons with color sparseness index less than 0.7 to each color at each luminance level. The responses of each neuron were normalized by the response to the most-preferred color of the same neuron (Fig. 8). Although the responses to bright red tended to be weak, there was no remarkable deference between the average normalized responses to each color, and this indicates that the neurons having sharp color tuning in PITC represent the entire color space as a whole.

Retinotopic organization of PIT

It was reported that the lateral surface of PIT has crude retinotopic organization (Boussaoud et al. 1991). To examine whether our recorded region also has retinotopy, we mapped the RFs of many neurons to examine how they distributed across the recorded area. In Fig. 9A, the RF of the recorded neurons are overlaid within the circles plotted at the coordinates of electrode penetration. The center of each circle indicates foveal center, and the edge corresponds to 20 degrees in eccentricity. When the RF extended outside the circle, the border of RF was shaded to indicate which part is inside of RF. A small number of neurons did not respond to the stimulus presented at the fovea, although their RF border enclosed the foveal center (the RF border drawn by dotted line). The position and extent of the RF varied depending on the recorded site. In dorsal half of the recorded region, most neurons had relatively small RFs enclosing foveal center. In ventral part, the size of RF became larger and the RF center shifted out of fovea, and as a result, neurons represented more peripheral visual field. In the ventral part, we also found that neurons in the anterior part had the RFs mainly containing lower visual field and those in more posterior part had the RFs mainly containing upper visual field. These results suggest that there exist retinotopic organization. To confirm this, we classified the RF into four categories based on its position and extent and examined how each category of RFs distribute in our recording sites. The

four categories are “fovea”, “upper visual field”, “lower visual field”, and “horizontal meridian”, respectively (see Methods). We adopted such categorical procedure to examine the retinotopy because the center of large RFs could not be determined precisely and because it appeared that retinotopy must be rather crude even if it existed. In Fig. 9B the category of each RF is indicated by a symbol and plotted at the recorded coordinates of the grid. In the dorsal half of PITC, most RFs contained foveal center. In the ventral part of PITC, the RFs shifted to more peripheral visual fields and neurons with “RF in lower visual field” and those with “RF in upper visual field” were clearly segregated in the anterior and posterior part, respectively. However, out of PITC, many neurons had RFs containing foveal center and no systematic change in the position and size of RFs were observed. To further confirm that the RFs shifted to more peripheral visual field in the ventral part of PITC, the distribution of the RF center across the recorded sites is shown in Fig. 9C. There is clear tendency that neurons recorded from more ventral region had RF centers with larger eccentricity values. Overall, the retinopy we observed in PITC is consistent with the retinotopic organization of TEO reported by Boussaoud et al. (1991). They reported that the eccentricities of RFs in TEO increased from dorsal to ventral part, and that the anterior and posterior part of TEO represented lower and upper visual field, respectively. This organization is the same as the crude retinotopy we observed in PITC.

Results of recordings from PIT of another monkey

In monkey MA, we recorded neuron activities from lateral surface of PIT in both hemispheres. PMTS of this monkey was located more ventrally than that of monkey KM. In spite of this, in the first hemisphere (right hemisphere), we attached a recording chamber at a position where electrodes can be penetrated at or close to the right angle to the cortical surface (R in Fig. 2C), as was done for the first monkey (KM). As a result, we could not sufficiently map neurons' activity from the cortical region around PMTS. As is shown later, the results of the mapping from this hemisphere were different from those obtained from KM. We speculated that this may be related to the fact that PMTS is located more ventrally in this hemisphere than that of KM, and we attempted to sample neurons form the cortical region around PMTS more extensively in the second hemisphere (left hemisphere) of monkey MA. To do this, we attached recording chamber at more steep angle in more dorsal position such that electrodes can be penetrated through the region around PMTS (L in Fig. 2C). The results of mapping from this hemisphere of MA were consistent with those from KM. Because of this, for monkey MA, we will first present the results obtained from the left hemisphere and then describe the results from the right hemisphere.

In the left hemisphere of monkey MA, electrodes were advanced obliquely in the cortex for a long distance (Fig. 2C) and an example of electrode track is shown in Fig. 10A. So, the coordinates on the grid is not a good indicator of the recorded position on the cortical surface. Therefore in this hemisphere, we constructed two-dimensional unfolded map of the recorded sites (Fig. 10) based on the X-ray picture of the electrode and the MRI image of the brain. We took X-ray picture at the end of each recording session with the electrode left in the brain and overlaid this X-ray picture with the MRI section to identify the position of electrodes in the brain. We mapped the distribution of neuron's selectivity (Fig. 10B), sparseness indices (Fig. 10C), and RFs (Fig. 10D) on the two-dimensional map. As expected, recording sites of the neurons included cortical regions inside and both dorsal and ventral to PMTS. Of these areas, the area within PMTS contained many color selective neurons with sharp color tuning and had crude retinotopy, and we consider this region corresponds to PITC identified in monkey KM (Fig. 10C and D, surrounded by dotted line: PITC). Within PITC, the dorsal part represented fovea, and in the ventral part, anterior region represented lower visual field, and the posterior region represented upper visual field, respectively (Fig. 10D). This pattern of visual field representation is consistent with that of PITC in monkey KM as shown in Figure 9.

The results of the quantitative analysis of color selectivity in the left hemisphere of monkey MA resembled that of monkey KM. The distribution of the color selectivity index and color sparseness index of the neurons in PITC (Fig. 11A, B) was similar to that of PITC neurons in monkey KM (Fig. 8A, B). Also, the distribution of these indices of the neurons recorded out of PITC (Fig. 11C, D) was similar to that of the neurons recorded out of PITC in monkey KM (Fig. 8C, D). In the left hemisphere of MA, there were differences in shape selectivity between PITC and the region out of PITC as well: PITC neurons (Fig. 11E, F) tended to have weaker and broader shape selectivity than the neurons recorded out of PITC (Fig. 11G, H).

In the right hemisphere of monkey MA, electrodes were penetrated roughly perpendicular to the cortical surface. Because the grid coordinates are good indicator of the recording sites of neurons, we will present the distribution of response properties using the grid coordinates (Fig. 12). PMTS was located slightly more ventral to the recording chamber in this hemisphere, and only a small part of PMTS was contained within the recording site. We found many color-selective neurons in the recorded sites, and many of them had shape selectivity as well. While many neurons had broad color tuning, there was some tendency that neurons recorded from more ventral part had smaller sparseness index values. Although this appears consistent with the observation in other two hemispheres, we did not find any clear pattern of visual field representation in this hemisphere. Neurons having RFs

containing foveal center were more or less intermingled with those representing upper or lower visual field (Fig. 12C). Because of this, we could not identify PITC in the right hemisphere of MA.

In this hemisphere, we present the results of quantitative analyses of color and shape selectivity without distinguishing two regions, namely PITC and the region out of PITC. Many neurons had broad tuning in both color and shape selectivity and the distribution of these indices are similar to those of neurons recorded from the region out of PITC in other two hemispheres rather than those recorded from PITC (Fig. 13A, > 0.6: n = 67, <= 0.6: n = 15, Fig. 13B, <= 0.7: n =29, > 0.7: n =53, Fig. 13C, > 0.6: n = 61, <= 0.6: n = 17, Fig. 13D, <= 0.7: n =28, > 0.7: n =50). Because we tended to found sharply color-tuned neurons at the most ventral part of the chamber, we speculate that the recorded sites in the right hemisphere of monkey MA contained only the dorsal edge of PITC. This possibility is suggested by the fact that we have obtained many color-selective neurons having sharp color tuning and crude retinotopy when electrode has been penetrated to proceed more ventrally in the left hemisphere of MA. From these results, we presume that PITC exists in a cortical region around PMTS and its position may shift with the variation of the location of PMTS between individual hemispheres.

Effects of the luminance contrast on the color-selective responses

We tested color selectivity by using sets of color stimuli with two different luminance contrasts for many neurons (see Methods), and found that responses often changed depending on the luminance contrast of the stimuli. Figure 14A illustrates the color selectivity of three example color-selective neurons tested by using colors brighter and darker than the background. In the upper row, the responses to colors in each luminance level are plotted on color space. In the lower row, the relationships between responses to dark (abscissa) and bright (ordinate) color stimuli at the same chromaticity coordinates are indicated as scatter plot. The neuron shown in a) had similar selectivity for bright and dark colors. As can be expected from similar color selectivities, this neuron showed strong positive correlation between the responses at two luminance conditions (r = 0.95). The neuron shown in b) selectively responded to yellow colors at either luminance levels, but the color selectivity obtained by the dark color stimuli was sharper than that obtained by the bright color stimuli. Consequently, the responses to two color stimulus sets showed moderate positive correlation (r = 0.63). The neuron in c) had quite different though overlapping color selectivity between bright and dark stimuli, and the preferred color was shifted from cyan to green. As a result, this neuron showed very weak correlation between

the responses to two sets of color stimuli (r = 0.13). We recorded and compared the responses at two luminance levels in 40 neurons recorded from PITC of monkey KM. Figure 14B shows the relationship between the maximum response for the bright color set (abscissa) and that for the dark color set (ordinate) for these 40 neurons. As the entire population, there was moderate correlation between the two set of responses (r = 0.53), but some of them showed quite different response magnitudes between the bright and dark color stimuli. In 11 out of these 40 neurons, the maximum response to one of the stimulus set (3 for bright colors, 8 for dark colors) was either less than 10 spikes/s or not significantly different from the background activity (t-test, $p > 0.05$). For the remaining 29 neurons, we calculated the correlation coefficient between the responses to the bright and dark color stimulus sets in order to examine the similarity of color selectivity between different luminance contrasts for each neuron. The distribution of the correlation coefficients is indicated in Fig. 14C. All neurons had positive correlation except for one neuron, but the correlation coefficient widely distributed from 0 to 1. This result indicates that, in PITC, the stability of color selectivity across different luminance contrasts varies from neuron to neuron.

The analysis above showed that color selectivity may change depending on the luminance contrast in PITC. This indicates the possibility that response of a neuron to colors with the same chromaticity coordinate may be influenced by the luminance contrast of the stimulus. So, we examined whether the effect of luminance contrast differs across different colors. To do this, for each of the 15 color set and neutral gray, we computed the correlation coefficients between the responses to dark and bright colors across the population of 29 PITC neurons that responded to both sets of colors. We found that the strength of correlation differed among colors. The results of this analysis conducted for red (Fig. 1A, No. 5) and neutral gray (Fig. 1A, W) are shown in Fig. 15A and B, respectively. For red color, there was clear positive correlation (r = 0.87), whereas the responses to gray showed slightly negative correlation (r = -0.14). The correlation coefficient for each of 16 colors are indicated by bar graph in Fig. 15C. There were strong positive correlations for the colors No. 4, 5, 9, and 15, while correlations were weak for colors No. 6, 7, 8 and 11, and even slightly negative for neutral gray (W). These differences in the strength of correlation occurred in a regular fashion within color space. In Fig.15D, the magnitudes of correlation coefficient between the responses to dark and bright colors are indicated by the diameter of circles and plotted at the corresponding chromaticity coordinates. Strong correlation tended to occur for colors with higher saturation, in particular red and blue, indicating that responses were stable for these colors regardless of the change in luminance contrast. On the other hand, correlation was weak and the responses tended to vary at different

luminance contrasts for colors with low saturation. Such tendency seems to correspond to our color perception well (see Discussion).

DISCUSSION

In the present study, we systematically investigated the color selective responses in PIT cortex at a cellular level. We recorded neuron activities from PIT and found that there exist many color selective neurons in this area. Previous electrophysiological study reported that some color-selective neurons exist in this area (Tanaka et al. 1991), and imaging studies have shown that PIT cortex was activated by color stimuli (Takechi et al. 1997; Tootell et al. 2004; Conwey and Tsao 2005). The results of the present study are consistent with these previous reports. However, to our knowledge, the present study is the first systematic attempt to examine the color selective responses of PIT neurons using color stimuli defined based on the color space and to examine the distribution of color selective properties of neurons in PIT.

We found that neurons having sharp color tuning were not homogeneously distributed in PIT, instead, they were concentrated in a certain region of PIT which we named PITC. Neurons located out of PITC had broader color tuning than those within PITC. A previous 2-DG experiment has shown that color stimulus evoked activation in patchy regions in PIT (Tootell et al. 2004), and our present result seems to be consistent with this report. These results suggest that PIT contains a domain which has distinct functional role in color vision. It has been shown that IT cortex has columnar organization in which neurons having similar stimulus selectivity are arranged in a column perpendicular to the cortical surface and that it forms a functional unit (Fujita et al. 1992). The dimension of each column in IT cortex is thought to be approximately 500 um along the cortical surface. On the other hand, PITC identified in the present study and the patchily activated region shown by Tootel et al. (2004) extends several millimeters and are clearly much larger than the size of an IT column. PITC can contain many columns within it. Recently, fMRI experiments in monkeys have reported the presence of regions of several millimeters in extent selectively responsive to faces (Logothesis et al.1999; Tsao et al. 2003; Tsao et al. 2006) or body parts (Tsao et al. 2003), and neural recordings confirmed this (Tsao et al. 2006). PITC may be conceived of as one of such regions with similar order of size and concentration of sharply color-tuned neurons.

We mapped the RFs in PIT and found that there was crude retinotopic organization in PITC. PITC can be clearly separated from V4 because of the large RF sizes and the location which is anterior to IOS. Neurons in the dorsal part of PITC had RFs containing the foveal center. In the ventral part, the eccentricity of RF increased and the RFs in the anterior and posterior part represented lower and upper visual field, respectively. This retinotopy corresponded well to what Boussaoud et al. (1991) reported in PIT. They conducted RF mapping from

PIT and reported that the retinotopic map covered the entire region of the lateral surface of PIT cortex ventral to STS, and named this area TEO. In our present study, we found that clear retinotopic organization was restricted within a part of PIT and this area corresponded to the region where neurons having sharp color selectivity were concentrated, namely PITC. Moreover, the position of the retinotopic map differed between individual hemispheres, and the positional shift seemed to be in coincident with the variation of the position of PMTS. These results strongly suggest that there is a circumscribed region in and around PMTS that has crude retinotopic organization and that is involved in the processing of color information. As we couldn't identify the ventral border of PITC, we need further investigation to know whether the overlap between the region with neurons having sharp color tuning and the region with crude retinotopic organizaiton continues in more ventral cortical region. Recently, Conway and Tsao (2005) reported in an fMRI experiment that the area on the posterior bank of STS responded to color stimuli and called the area PITd (Van Essen et al. 1990). Our recorded sites were out of STS and they are clearly different from PITd. It is interesting to know the color selective properties of neurons in PITd and how they differ from those in PITC.

In the present study, we also tested the shape selectivity of neurons. We found that many neurons were selective to both color and shape, and that shape selective neurons distributed across the entire PIT cortex we examined. This result is consistent with previous findings that there were many shape selective neurons in PIT (Tanaka et al. 1991; Brincat and Connor 2004) and that the ablation of this area caused severe deficit in pattern discrimination (Iwai and Mishkin 1969). Within PITC, we also found that color-selective neurons with and without shape selectivity were intermingled. This suggests that the processing of color information and shape information takes place in close relationship in PIT. In area TE, we have observed that the color-selective neurons without shape selectivity were concentrated in a region slightly lateral to the anterior middle temporal sulcus (AMTS). The difference in such distributing pattern between PIT and TE may reflect different functional roles between these two areas. Recently, we have reported that the color-selective TE neurons are strongly activated when the monkeys performed categorical color judgement (Koida and Komatsu 2007). This suggests that TE has an important role in associating color information and behavior. On the other hand, the close relationship between the processing of color and shape information in PIT may imply that PIT may be an important stage where color information is added to shape information to construct an object image.

Previous studies have shown that lesion of PIT in monkeys affected the ability of pattern discrimination (Iwai and Mishkin 1969) and visual attention (De weed et al. 1999). With

regard to color vision, there has been no study showing clear deficit in the performance of color discrimination by PIT lesion. Huxlin et al. (2000) reported that the threshold of color discrimination is not influenced when the lesion was restricted to PIT. On the other hand, a number of studies have shown that the lesion of the entire IT cortex or area TE caused deficit in the performance of color discrimination (Horel 1994; Heywood and Cowey 1995; Buckley et al. 1997; Huxlin et al. 2000; Cowey et al. 2001). Combining these results, we can think that TE plays an essential role in color discrimination and that color information can be conveyed to area TE even when PIT cortex is damaged. It has been shown that V4 neurons project to the posterior part of TE (Van Essen et al. 1990). It can be thought that this projection plays an important role when the monkey with damage in PIT performs color discrimination. If so, we can predict that the performance of color discrimination will be severely deteriorated by the combined lesion of both V4 and PIT even though lesion of each area alone does not cause clear deficit in color discrimination.

The luminance contrast between the stimulus and background is an important factor in color perception. In the present study, we examined the effect of luminance contrast on the responses to color stimuli by using color stimulus sets at two luminance contrasts. We found many PITC neurons changed their responses to color stimuli depending on their luminance contrasts. In addition, when we considered the color representation with the activities of the entire population of neurons, we found that the responses to red and blue were stable across two luminance contrasts while the responses to less-saturated colors were variable with the change in luminance contrast. This seems consistent with the fact that the perceived color of un-saturated colors significantly change such as white, gray, and black depending on the luminance contrast whereas that of blue and red do not change by the change in the luminance contrast (Uchikawa et al. 1989). No study tested systematically wether the neuron's response is changed depending on its luminance contrast. Yoshioka et al. (1996) recorded from V1, V2 and V4 and reported that the neuron's responses to endspectral color (red and blue, etc.) are stable between two luminance conditions (brighter than and equiluminant to background) while the responses to midspectral color (for example, yellow) are unstable. However, they did not test the luminance effect on neuron's response when the luminance contrast was reversed. So, whether the effects of the luminance contrast on the color-selective responses we found in PITC is derived from the early visual areas or newly created in PITC is an interested question to be addressed in future.

REFERENCES

Bonin, G.V. & Bailey, P. (1947) “The Neocortex of *Macaca Mulatta*.” University of Illinois Press, Urbana.

Boussaoud, D., Desimone, R. & Ungerleider, L.G. (1991) Visual topography of area TEO in the macaque. *J. Comp Neurol*., 306, 554-75.

Brincat, S.L. & Connor, C.E. (2004) rlying principles of visual shape selectivity in posterior inferotemporal cortex. *Nat. Neurosci*., 7, 880-6.

Buckley, M.J., Gaffan, D. & Murray, E.A. (1997) Functional double dissociation between two inferior temporal cortical areas: perirhinal cortex versus middle temporal gyrus. *J. Neurophysiol*., 77, 587-98.

Cowey, A., Heywood, C.A. & Irving-Bell, L. (2001) The regional cortical basis of achromatopsia: a study on macaque monkeys and an achromatopsic patient. *Eur. J. Neurosci*., 14, 1555-66.

Conway, B.R. & Tsao, D.Y. (2005) Color Architecture in Alert Macaque Cortex Revealed by fMRI. *Cereb. Cortex*., 16, 1604-13.

Crist ,C.F., Yamasaki, D.S., Komatsu, H. & Wurtz, R.H. (1998) A grid system and a microsyringe for single cell recording. *J. Neurosci Methods*., 26, 117-22.

De Weerd, P., Peralta, M.R., Desimone, R. & Ungerleider, L.G. (1999) Loss of attentional stimulus selection after extrastriate cortical lesions in macaques. *Nat. Neurosci.,* 2, 753-8.

Fujita, I., Tanaka, K., Ito, M. & Cheng, K. (1992) Columns for visual features of objects in monkey inferotemporal cortex. *Nature*., 360, 343-6.

Heywood, C.A., Gaffan, D. & Cowey, A. (1995) Cerebral achromatopsia in monkeys. *Eur. J. Neurosci*., 7, 1064-73.

Horel, J.A. (1994) Retrieval of color and form during suppression of temporal cortex with cold. *Behav. Brain Res*., 65, 165-72.

Hubel, D.H. & Livingstone, M.S. (1987) Segregation of form, color, and stereopsis in primate area 18. *J. Neurosci*., 7, 3378-415.

Huxlin, K.R., Saunders, R.C., Marchionini, D., Pham, H.A. & Merigan, W.H. (2000) Perceptual deficits after lesions of inferotemporal cortex in macaques. *Cereb. Cortex*., 10, 671-83.

Iwai, E. & Mishkin, M. (1969) Further evidence on the locus of the visual area in the temporal lobe of the monkey. *Exp. Neurol*., 25, 585-94.

Koida, K. & Komatsu, H. (2007) Effects of task demands on the responses of color-selective neurons in the inferior temporal cortex. *Nat. Neurosci*., 10, 108-16.

Komatsu, H. & Ideura, Y. (1993) Relationships between color, shape, and pattern selectivities of neurons in the inferior temporal cortex of the monkey. *J. Neurophysiol*., 20, 677-94.

Komatsu, H., Ideura, Y., Kaji, S. & Yamane, S. (1992) Color selectivity of neurons in the inferior temporal cortex of the awake macaque monkey. *J. Neurosci*., 12, 408-24.

Logothetis, N.K., Guggenberger, H., Peled, S. & Pauls, J. (1999) Functional imaging of the monkey brain. *Nat. Neurosci*., 2, 555-62.

Robinson D.A. (1963) A method of measuring eye movement using a scleral search coil in a magnetic field. *IEEE Trans Biomed Eng*., 10, 137-45.

Rolls, E.T. & Tovee, M.J. (1995) Sparseness of the neuronal representation of stimuli in the primate temporal visual cortex. *J. Neurophysiol*., 73, 713-26.

Schein, S. & Desimone, R. (1990) Spectral properties of V4 neurons in the macaque. *J. Neurosci*., 10, 3369-89.

Takechi, H., Onoe, H., Shizuno, H., Yoshikawa, E., Sadato, N., Tsukada, H. & Watanabe, Y. (1997) Mapping of cortical areas involved in color vision in non-human primates. *Neurosci. Lett*., 230, 17-20.

Tanaka, K., Saito, H., Fukada, Y. & Moriya, M. (1991) Coding visual images of objects in the inferotemporal cortex of the macaque monkey. *J. Neurophysiol*., 66, 170-89.

Tootell, R.B., Nelissen, K., Vanduffel, W. & Orban, G.A. (2004) Search for Color 'Center(s)' in Macaque Visual Cortex. *Cereb. Cortex*., 14, 353-363.

Tsao, D.Y., Freiwald, W.A., Knutsen, T.A., Mandeville, J.B.,Tootell, R.B., Boussaoud, D., Desimone, R. & Ungerleider, L.G. (2003) Faces and objects in macaque cerebral cortex. *Nat. Neurosci*., 9, 989-95.

Tsao, D. Y., Freiwald, W. A., Tootell, R. B. & Livingstone, M. S. (2006) A cortical region consisting entirely of face-selective cells. *Science*., 311, 670-4.

Uchikawa, H., Uchikawa, K. & Boynton, R.M. (1989) Influence of achromatic surrounds on categorical perception of surface colors. *Vision. Res*., 29, 881-90.

Van Essen ,D.C., Felleman, D.J., DeYoe, E.A., Olavarria, J. & Knierim J. (1990) Modular and hierarchical organization of extrastriate visual cortex in the macaque monkey. Cold Spring Harb Symp Quant Biol., 55, 679-96.

Yoshioka, T., Dow, B.M., Vautin, R.G. (1996) Neuronal mechanisms of color categorization in areas V1, V2 and V4 of macaque monkey visual cortex. Behav Brain Res., 76, 51-70.

Zeki, S. (1973) Colour coding in rhesus monkey prestriate cortex. *Brain Res*., 53(2), 422-7.

LEGENDS

Fig. 1

A, Standard set of colors used to test color selectivity. The chromaticity coordinate of each color is indicated by a spot on the CIE 1931 chromaticity diagrams. R, G, B indicate the positions of the 3 primary colors of the monitor we used in the experiments. Test colors are 15 colors that covered evenly the portion of the color space delimited by three primary colors. In some experiments we additionally used a neutral gray (W). ***B***, Standard sets of 11 geometric shapes used to test shape selectivity: square, diamond, circle, star, cross, oblique cross, triangle, vertical bar, oblique bar in clockwise direction, horizontal bar and oblique bar in counterclockwise direction. During testing, each shape stimulus was painted homogeneously with the same color.

Fig. 2

A, Lateral view of the left hemisphere of a monkey (KM). The areas involved in the ventral stream are indicated. Inferior temporal (IT) cortex is divided into three parts; AIT, anterior IT; CIT, central IT; PIT, posterior IT. PIT extends from the rostral edge of IOS to the rostral edge of PMTS in antero-posterior direction. Black square indicates the area covered by the recording chamber used for monkey KM. ***B*** and ***C***, MRI images of the coronal section of the recorded hemispheres including PIT. The stereotaxic coordinate is anterior 3mm in ***B*** and 6mm in ***C***. ***B***, Left hemisphere of monkey KM. ***C***, Left (L) and right (R) hemispheres of monkey MA. Position and size of the recording chambers used are indicated by a white line. Positions of STS and PMTS in each hemisphere are indicated by white and black arrowheads, respectively. In both hemispheres of monkey MA, PMTS is located in more ventral part than in monkey KM. AMTS, anterior middle temporal sulcus; IOS, inferior occipital sulcus; LS, lunate sulcus; PMTS, posterior middle temporal sulcus; STS, superior temporal sulcus; A, anterior; D, dorsal; P, posterior; V, ventral.

Fig. 3

Recording sites of monkey KM and the distribution of color/shape selectivities. ***A***, Enlarged view of the recording sites shown on the brain of monkey KM. A red square indicates the area covered by the recording chamber. To confirm the position of the recording chamber, we made markings of electrode tip by electrolytic deposition of iron of elgiloy microelectrode in some tracks. An arrow indicates a penetrated site where one of these markings was conducted. ***B***, Coronal section of the PIT of monkey KM stained by Cresyl Violet containing one of markings indicated by an arrow. This is the same marking as shown in ***A***.

C, Stimulus selectivity of neurons across the surface of the PIT cortex. The stimulus selectivity of each neuron is indicated by symbols and plotted at the coordinate of penetration sites within the grid where the responses were recorded. Open circles indicate the hole of the grid used for electrode penetrations. Red symbol indicates that a neuron was color selective, and black symbol indicates not color-selective. Star indicates that a neuron was shape selective, and circle indicates not shape-selective. Open stars indicate neurons that preferentially responded to either a black or white stimulus. Thick and pale symbols indicate that the stimulus selectivity was determined quantitatively and qualitatively, respectively. An arrow indicates the site where electrode marking shown in ***A*** and ***B*** was made. A dashed line indicates the presumable border between PIT and V4. Two recorded positions at the top right corner located on and at the extension of IOS were excluded from PIT. L, lateral; M, medial. Other abbreviations are the same as in Fig. 2. Scale bar, 5 mm in *A*, 1 mm in ***B*** and ***C***.

Fig.4

Color selectivity and shape selectivity of three example PIT neurons are shown in ***A***, ***B*** and ***C***, respectively. Histograms and rasters show the responses of the neuron to 15 colors and 11 shapes. Each stimulus was presented for 500 msec period that is indicated by the thick horizontal line below each histogram. Responses to color stimuli are shown on the top row, and those to shape stimuli are shown on the bottom row. The number of presented color and the shape of geometric stimulus is shown at the top left of each histogram. The number of color corresponds to that shown in Fig. 1A. To the right on the top row, response magnitudes to color stimuli are represented by diameters of circles and are plotted at positions that correspond to their chromaticity coordinates. Open and solid circles indicate excitation and inhibition, respectively. Contour lines indicate 75, 50, 25 and 0% of the maximum response. On the bottom row, responses to shape stimuli are plotted as a line graph.

Fig. 5

Color-selective responses of eight example PIT neurons. Responses to 15 colors are plotted in the same way as shown in Fig. 4. Six example neurons (***A*** - ***F***) that were recorded from postero-ventral two-thirds of the recording sites of monkey KM had sharp color tuning. The neuron shown in ***G*** is selective for several hues (from green to yellow and from purple to blue) and that in ***H*** had very broad color tuning. These examples were arranged according to the size of the sparseness index. From ***A*** to ***H***, the sparseness index of each neuron is 0.23, 0.41, 0.55, 0.61, 0.61, 0.65, 0.78, 0.97, respectively.

Fig. 6

The distribution of the color sparseness indices at each position of the grid in PIT of monkey KM. A number indicates the color sparseness index of one neuron and is indicated at the coordinate of penetration site within the grid where the response was recorded. The value less than 0.7 is marked with thick font. Neurons recorded from the postero-ventral two-third of the recording sites tended to have sharper color tuning: at the recording sites ventral to the dotted line, many neurons had sparseness index less than 0.7, whereas at the positions dorsal to the dotted line, few neurons did. We tentatively named the region ventral to the dotted line PITC (PIT color area). Numbers marked by alphabets (***A*** - ***H***) indicate neurons whose color selectivities are shown in Fig. 5.

Fig. 7

Distribution of the selectivity index and sparseness index for neurons in PITC (***A***, ***B***, ***E***, ***F***) and for those out of PITC (***C***, ***D***, ***G***, ***H***) recorded from monkey KM. Filled bars represent neurons with stimulus selectivity and open bars those without stimulus selectivity. ***A*** – ***D*** show the distribution of indices for color selectivity; color selectivity index (***A***, ***C***) and color sparseness index (***B***, ***D***). ***E*** – ***H*** show that for shape selectivity; shape selectivity index (***E***, ***G***) and shape sparseness index (***F***, ***H***). The panels in the top and the third rows include cells recorded within PITC and those in the second and the forth rows include cells recorded out of PITC. For the test of shape selectivity, three neurons in the PITC and four neurons outside the PITC were not tested by bar stimuli (see Methods). These seven neurons were excluded from the analysis of shape sparseness index.

Fig. 8

Average response of all PITC neurons with color sparseness index less than 0.7 to each color at each luminance level, recorded from monkey KM. For each neuron, the response to each color was normalized by the response to the most-preferred color of the same neuron. The left panel shows the responses to the sets of color stimuli at 5 cd/m^2 and the right panel shows the responses to those at 20 cd/m^2 (or 11 cd/m^2 for blue). At each luminance level, PIT neurons represented the entire color space as a population.

Fig. 9

Distribution of the receptive fields (RFs) recorded from PIT of monkey KM. ***A***, The RF of recorded neurons are overlaid within the circles plotted at the coordinates of electrode penetration. The center of each circle indicates foveal center, and the edge corresponds to 20 degree in eccentricity. When the RF extended outside the circle, the border of RF was

shaded to indicate which part is inside of RF. RFs indicated by rectangles indicate that the neurons responded at any location of visual field examined. RFs indiated by dashed line contained the foveal center, but the stimulus presented at the foveal center did not evoke neural response. In each panel, dashed line at the top-right indicates the border between V4 and PIT, and a dotted line indicates the border between PITC and the rest of PIT. ***B***, Classification of RFs into four categories according to the position and extent of the RFs. Symbols indicate the four categories of RFs; 'F' represents RF in the "fovea", an open circle for RF in the "upper visual field", a solid circle for RF in the "lower visual field", and a triangle for "RF over horizontal meridian", respectively. ***C***, Eccentricity of the RF center of each neuron. Eccentricity was obtained by calculating the distance between the foveal center and the RF center. Eccentricity of RF center is categorized into 5 classes and marked by different colors as shown at the bottom.

Fig. 10

Distribution of the color selectivity, shape selectivity and receptive fields in the PIT cortex of the left hemisphere of monkey MA. ***A***, Cresyl violet-stained coronal section of the PIT around the PMTS. ***B*** - ***C***, The data are plotted at the recording site of each neuron on the two- dimensional unfolded map. Solid lines indicate the ridge of sulci, and the broken line indicates the fundus of PMTS. The region inside the IOS (gray region) should be area V4, and neurons recorded in this region were excluded from the sample. ***B***, Distribution of color/shape selectivity of each neuron. Symbols are the same as in Fig. 3C. ***C***, Distribution of the sparseness indices. The index value < 0.7 is marked by red color. ***D***, Distribution of the RFs classified into the same four categories as in Fig. 9B. In ***B*** and ***C***, presumable border of PITC is enclosed by a dashed oval. Scale bar, 1mm.

Fig. 11

Distribution of the selectivity index and sparseness index for neurons in PITC (***A***, ***B***, ***E***, ***F***) and for those out of PITC (***C***, ***D***, ***G***, ***H***) recorded from the left hemisphere of monkey MA. The alignment of the data is in the same manner as in Fig. 7.

Fig. 12

Distribution of the color selectivity, shape selectivity and receptive fields in the PIT cortex of the right hemisphere of monkey MA. The data are plotted at the coorinate of the grid hole where the neuron was recorded. Gray circles indicate recording sites outside the PIT. ***A***, Distribution of color/shape selectivities. ***B***, Distribution of the sparseness indices. ***C***, Distribution of the RFs. All symbols and colors are the same as in Fig. 10. Abbreviations are

the same as in Fig. 3. Scale bar, 1 mm.

Fig. 13

Distribution of the selectivity indices and sparseness indices of the neurons recorded from the right hemisphere of monkey MA. ***A***, Distribution of the color selectivity indices. ***B***, Distribution of the color sparseness indices. ***C***, Distribution of the shape selectivity indices. ***D***, Distribution of the shape sparseness indices.

Fig. 14

Effects of the luminance contrast of stimuli on the color selective responses of PITC neurons. ***A***, Responses of three example PITC neurons to color stimuli darker (5 cd/m^2) and brighter (20 cd/m^2 or 11 cd/m^2 for blue) than the background (10 cd/m^2). 'a', 'b' and 'c' correspond to different neurons. For each neuron, color selectivity obtained at two luminance contrasts are shown at the top row in the same way as in Fig. 5. At the bottom row, relationship between the responses to dark (abscissa) and bright (ordinate) color stimuli at the same chromaticity coordinates are indicated as scatter plot. ***B***, The relationship between the maximum responses for the bright color set (abscissa) and that for the dark color set (ordinate) of 40 neurons recorded from PITC of monkey KM in which responses were recorded at two luminance levels. Dashed lines indicate where the responses are 10 spikes/s. ***C***, Distribution of the correlation coefficient between the responses to the bright and dark color stimulus sets for 29 PIT neurons in which responses to both color stimulus sets exceeded 10 spikes/s. .

Fig. 15

Effects of the luminance contrast on the population responses of PITC neurons to color stimuli. ***A*** and ***B***, Correlation coefficients between responses to dark and bright colors across the population of 29 PITC neurons that responded to both sets of colors. ***A*** is for red color, ***B*** is for gray color. Each point in the graph represents one neuron. ***C***, Magnitude of the correlation coefficient for each of the 15 colors in Fig. 1B and neutral gray (W). ***D***, The same data as shown in ***C*** is expressed as diameters of circles and are plotted at the position that corresponds to the chromaticity coordinates of the color to make it easier to see how the difference in the correlation occurred in the color space.

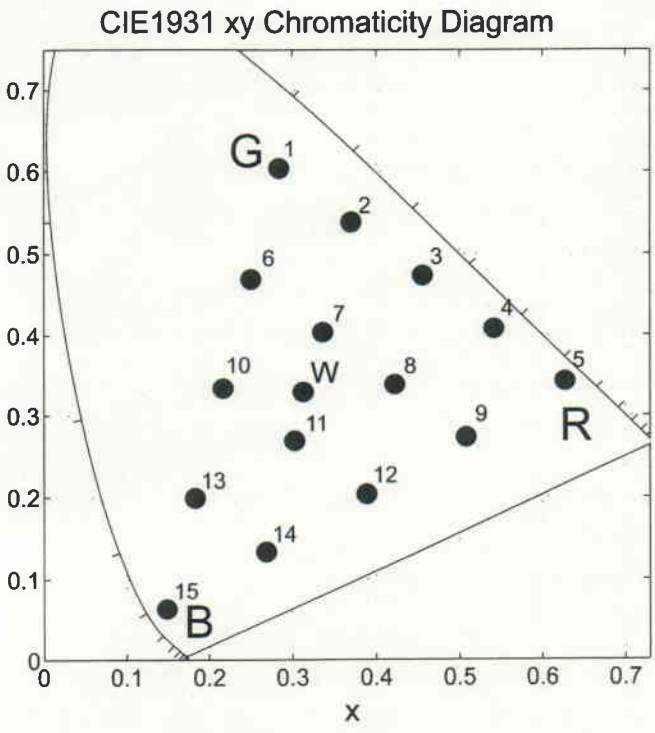
CIE1931 xy Chromaticity Diagram
G
1
2
3
4
5
6
7
8
9
10
W
11
12
13
14
15
B
R
0.7
0.6
0.5
0.4
0.3
0.2
0.1
0
0.1
0.2
0.3
0.4
0.5
0.6
0.7
x


B

Fig. 1

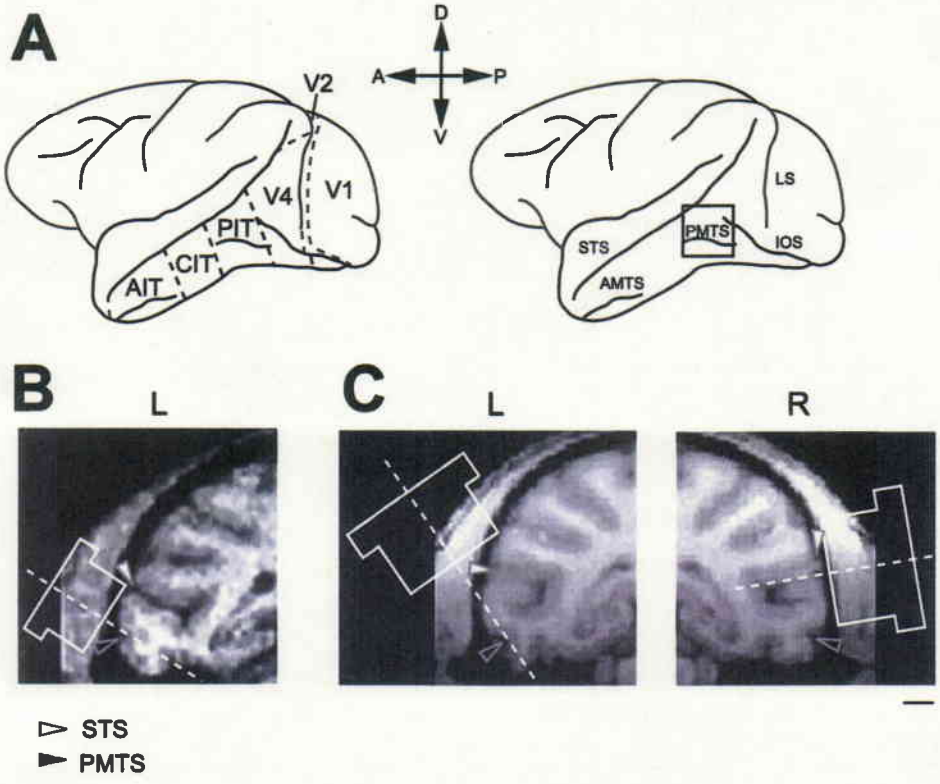

Fig. 2

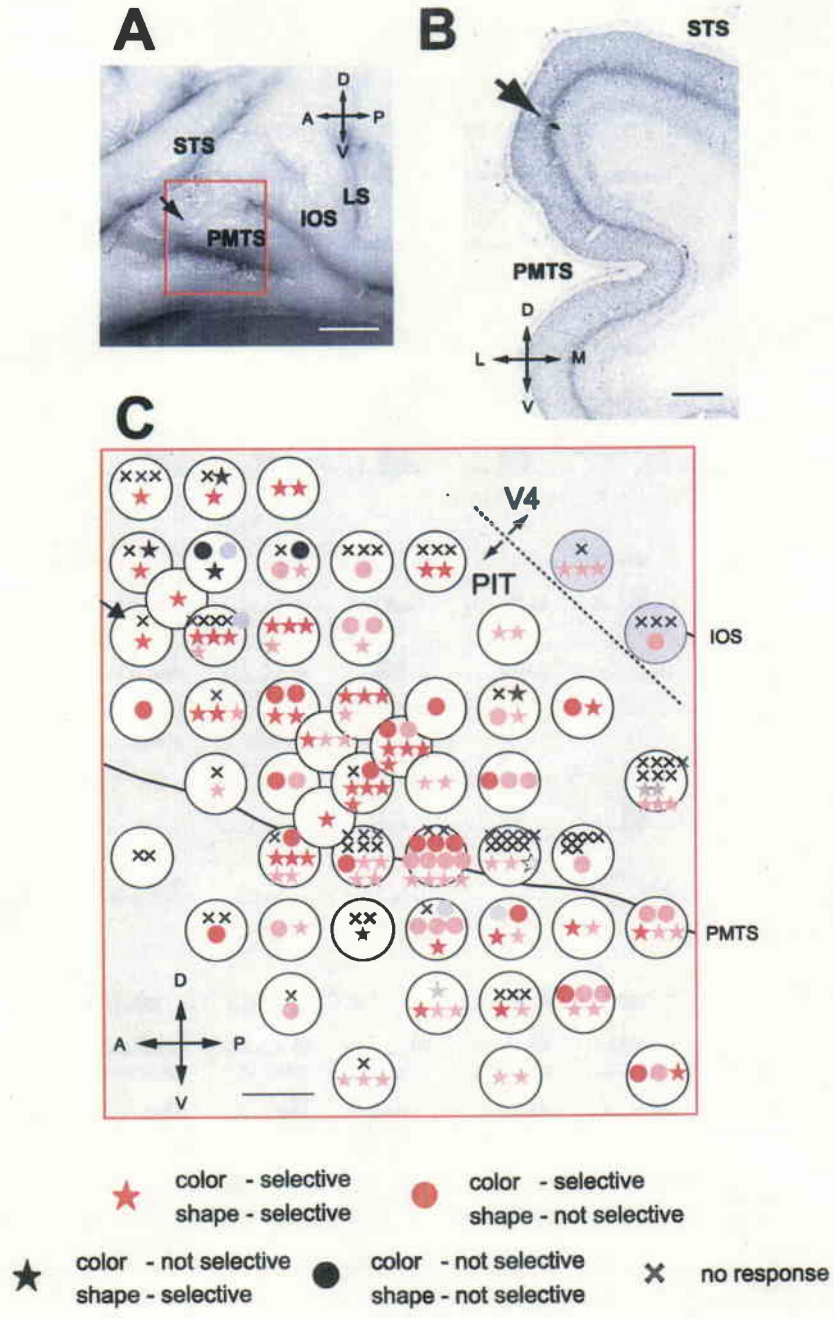
A
B
C
STS
LS
IOS
PMTS
D
A
P
V
L
M
V4
PIT
color - selective
shape - selective
color - selective
shape - not selective
color - not selective
shape - selective
color - not selective
shape - not selective
no response

Fig. 3

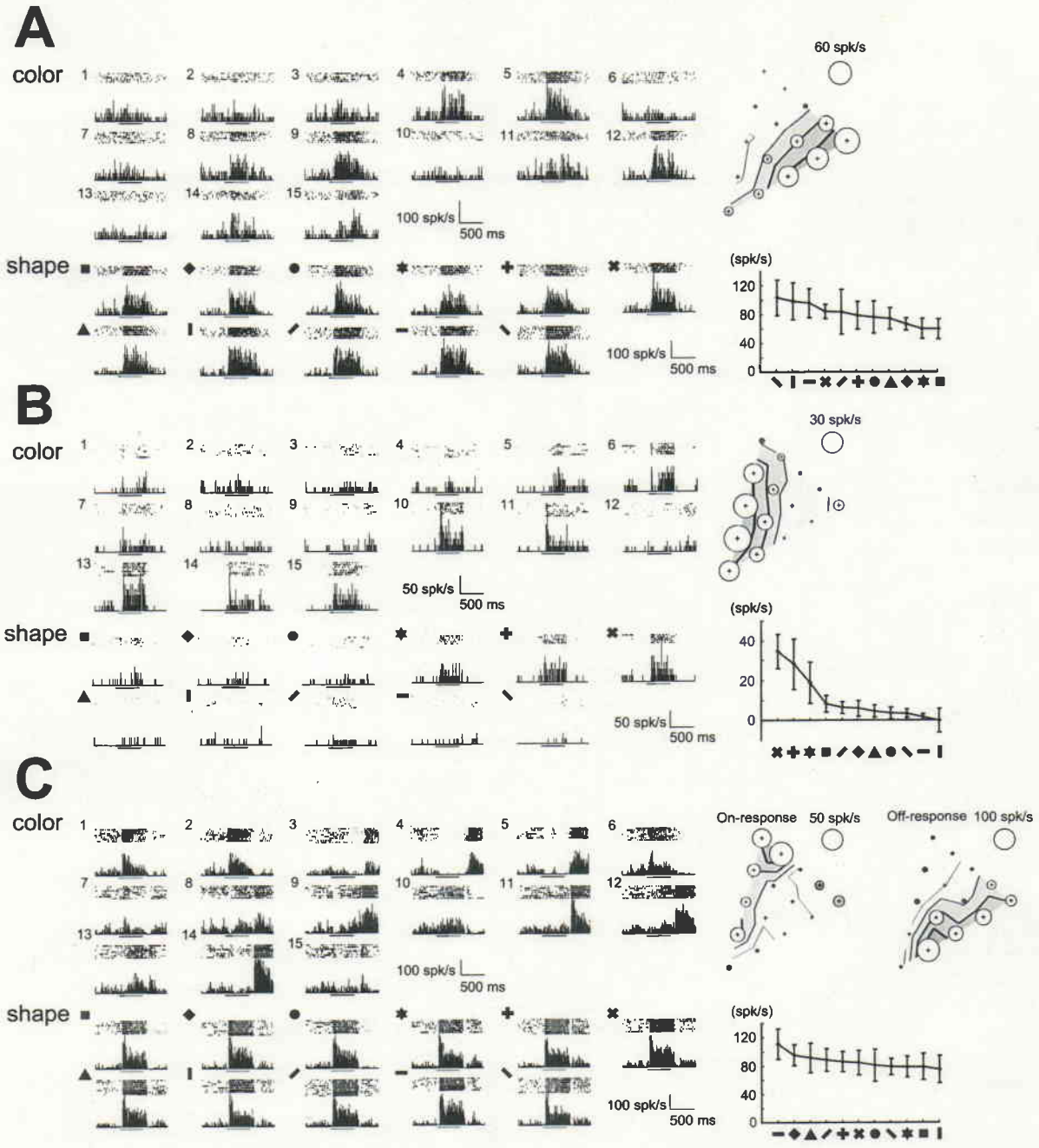
A
color
1
2
3
4
5
6
7
8
9
10
11
12
13
14
15
100 spk/s
500 ms
60 spk/s
shape
100 spk/s
500 ms
(spk/s)
120
80
40
0
B
color
30 spk/s
50 spk/s
500 ms
shape
50 spk/s
500 ms
(spk/s)
40
20
0
C
color
On-response 50 spk/s
Off-response 100 spk/s
100 spk/s
500 ms
shape
100 spk/s
500 ms
(spk/s)
120
80
40
0

Fig. 4

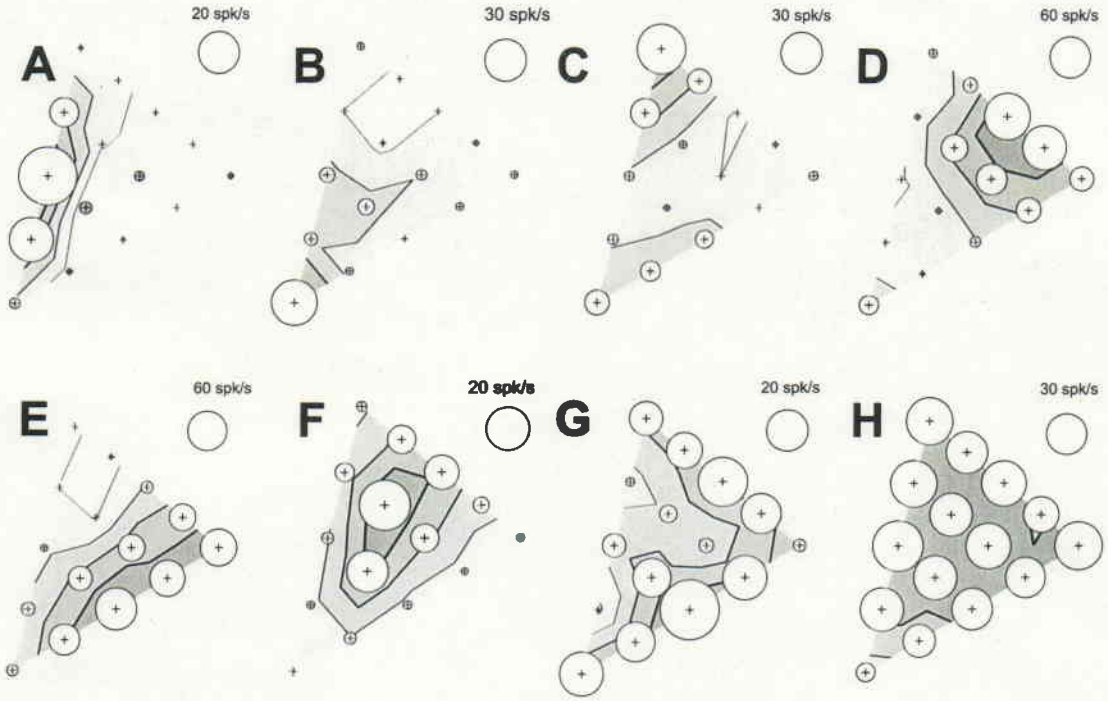
A
20 spk/s
B
30 spk/s
C
30 spk/s
D
60 spk/s
E
60 spk/s
F
20 spk/s
G
20 spk/s
H
30 spk/s

Fig. 5

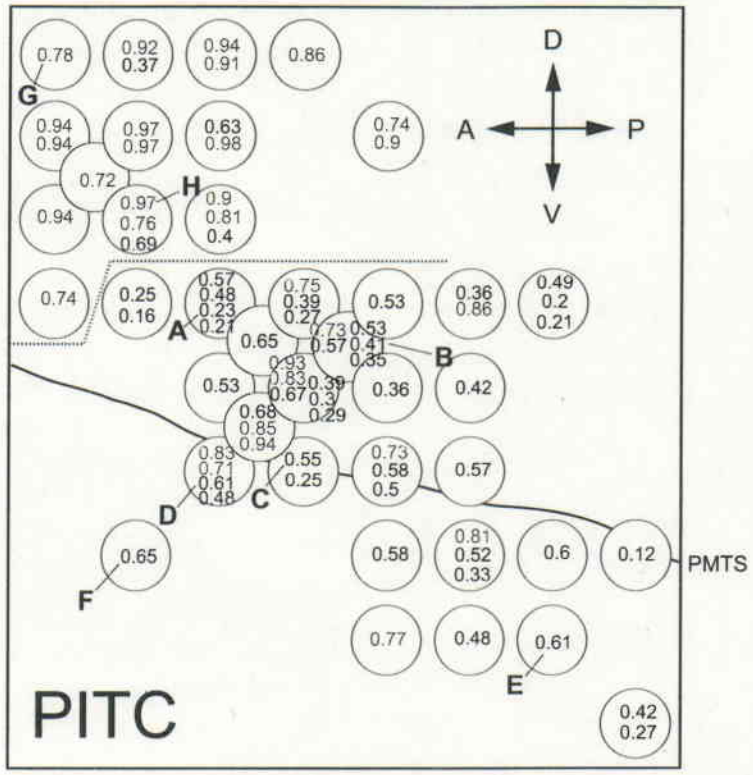

Fig. 6

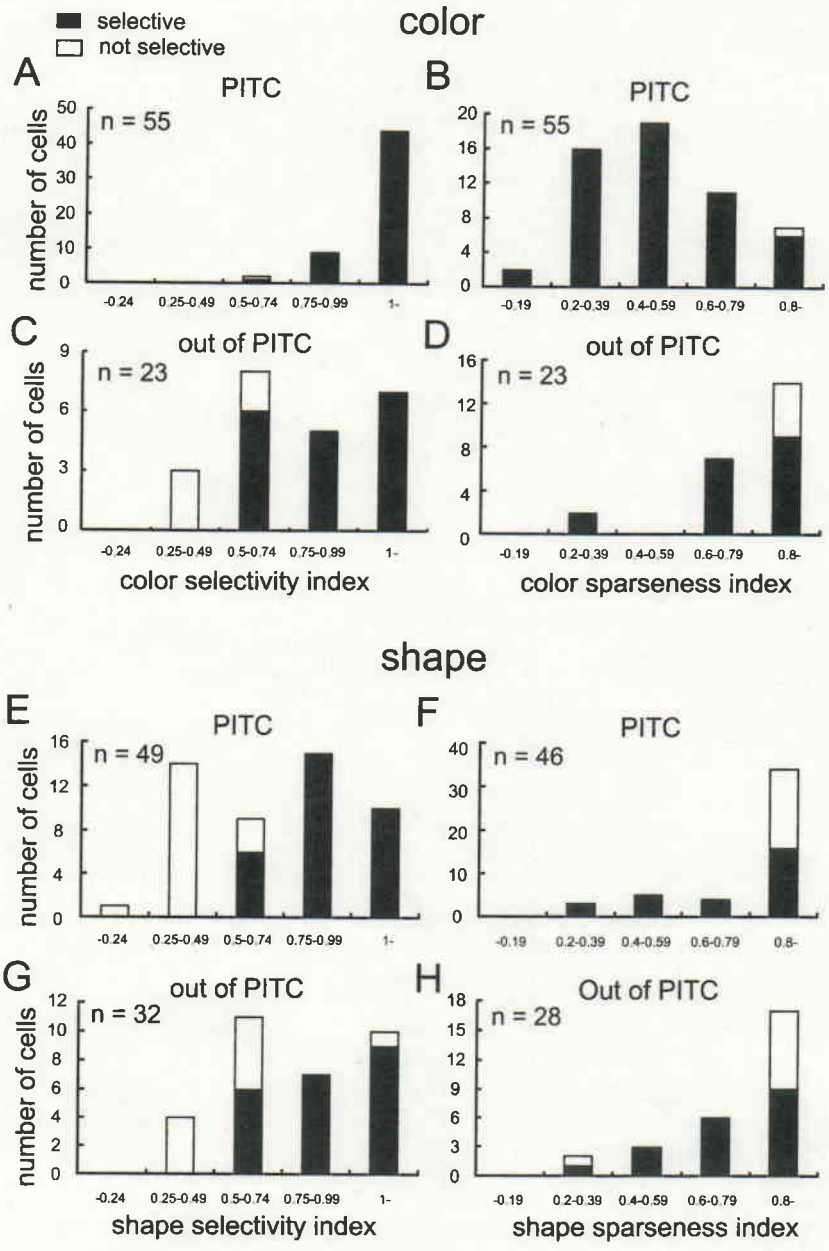
color
selective
not selective
A
PITC
n = 55
number of cells
-0.24
0.25-0.49
0.5-0.74
0.75-0.99
1-
B
PITC
n = 55
-0.19
0.2-0.39
0.4-0.59
0.6-0.79
0.8-
C
out of PITC
n = 23
color selectivity index
D
out of PITC
n = 23
color sparseness index
shape
E
PITC
n = 49
F
PITC
n = 46
G
out of PITC
n = 32
shape selectivity index
H
Out of PITC
n = 28
shape sparseness index

Fig. 7

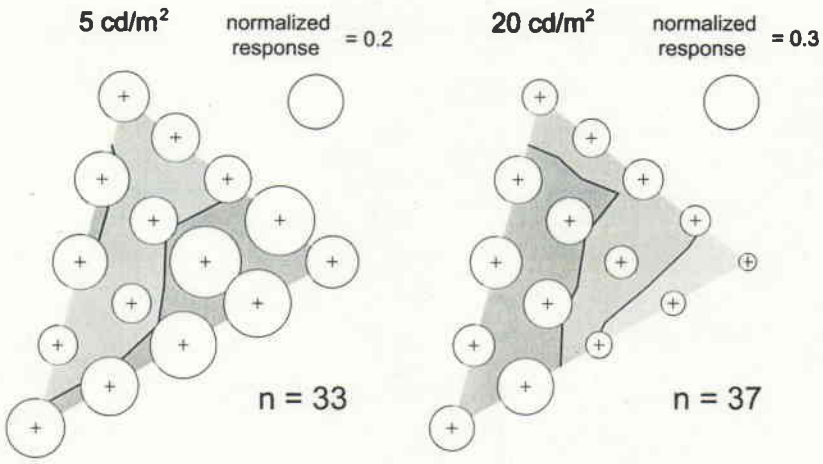
5 cd/m²
normalized response
= 0.2
n = 33
20 cd/m²
normalized response
= 0.3
n = 37

Fig. 8

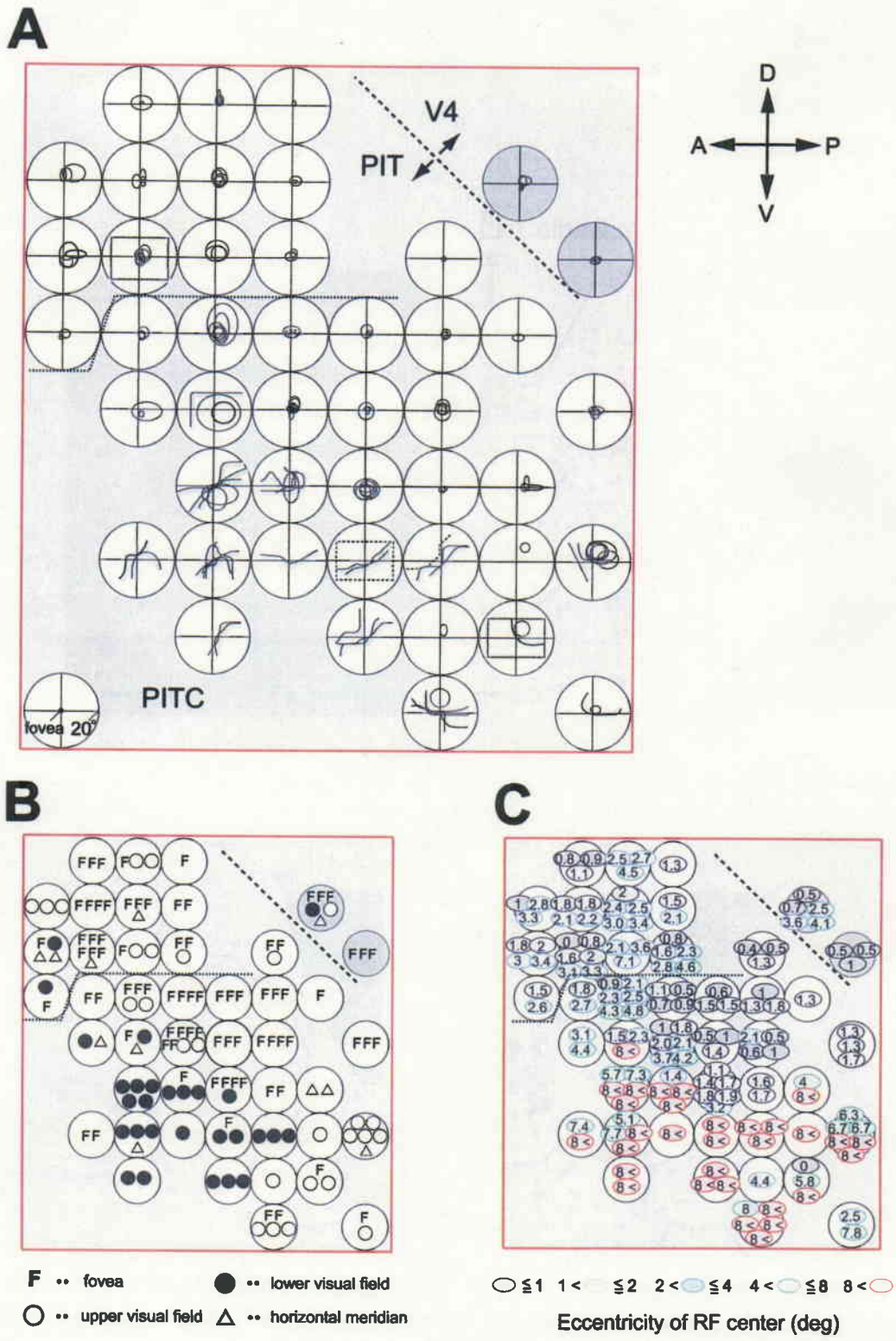
A
V4
PIT
PITC
fovea
20°
D
A
P
V
B
C
F •• fovea
•• lower visual field
•• upper visual field
•• horizontal meridian
≦1 1< ≦2 2< ≦4 4< ≦8 8<
Eccentricity of RF center (deg)

Fig. 9

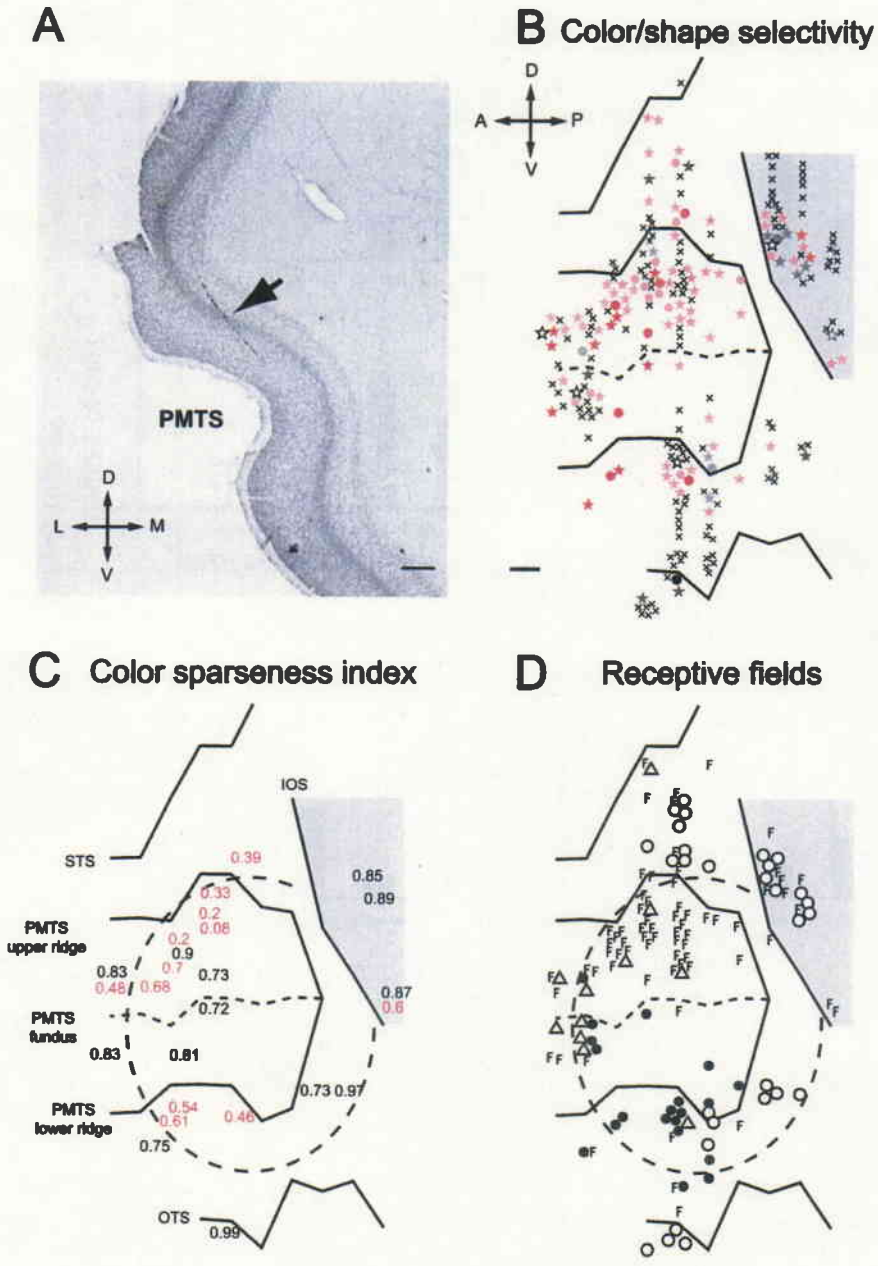
A
PMTS
D
L
M
V
B Color/shape selectivity
D
A
P
V
C Color sparseness index
IOS
STS
PMTS
upper ridge
PMTS
fundus
PMTS
lower ridge
OTS
0.39
0.33
0.2
0.08
0.2
0.9
0.7
0.83
0.48
0.68
0.73
0.72
0.83
0.81
0.54
0.61
0.46
0.75
0.99
0.85
0.89
0.87
0.6
0.73
0.97
D Receptive fields

Fig. 10

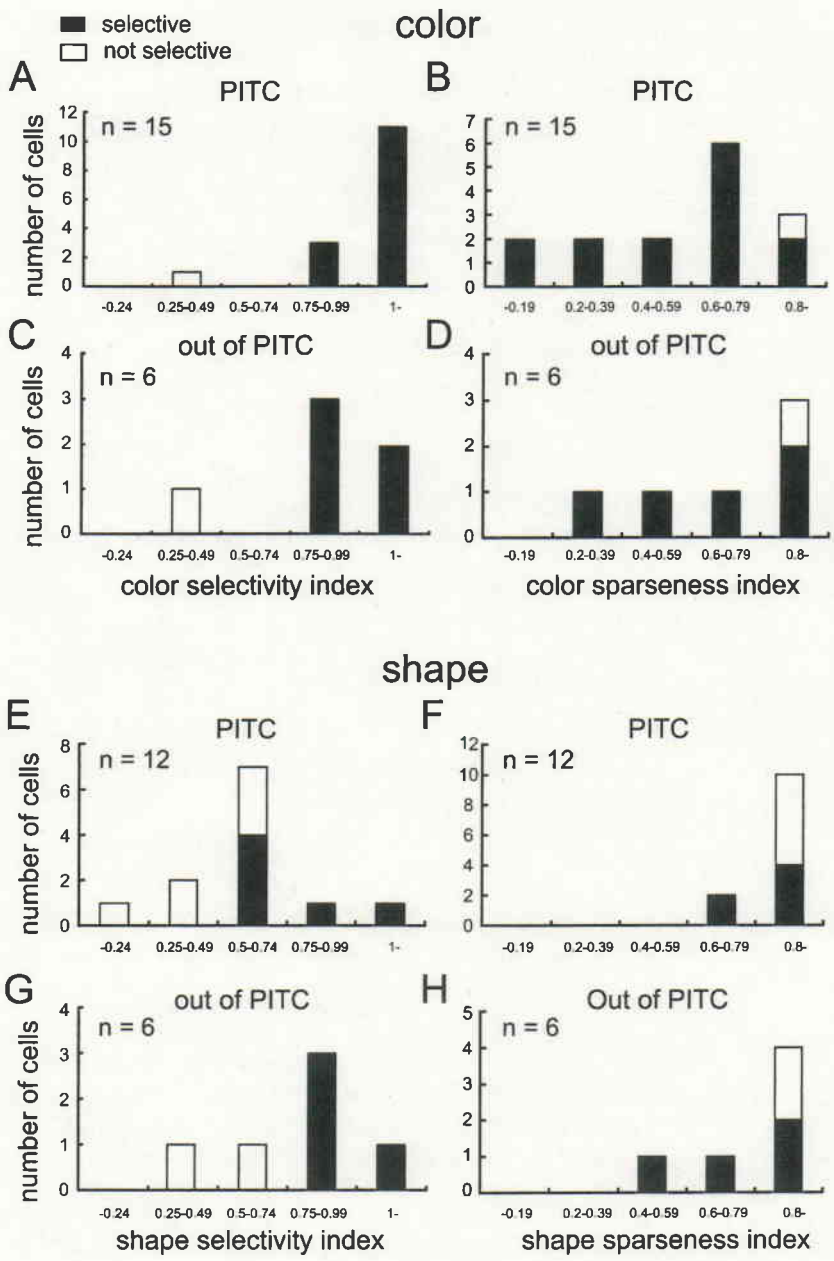
color
selective
not selective
A
PITC
n = 15
number of cells
-0.24
0.25-0.49
0.5-0.74
0.75-0.99
1-
B
PITC
n = 15
-0.19
0.2-0.39
0.4-0.59
0.6-0.79
0.8-
C
out of PITC
n = 6
color selectivity index
D
out of PITC
n = 6
color sparseness index
shape
E
PITC
n = 12
F
PITC
n = 12
G
out of PITC
n = 6
shape selectivity index
H
Out of PITC
n = 6
shape sparseness index

Fig. 11

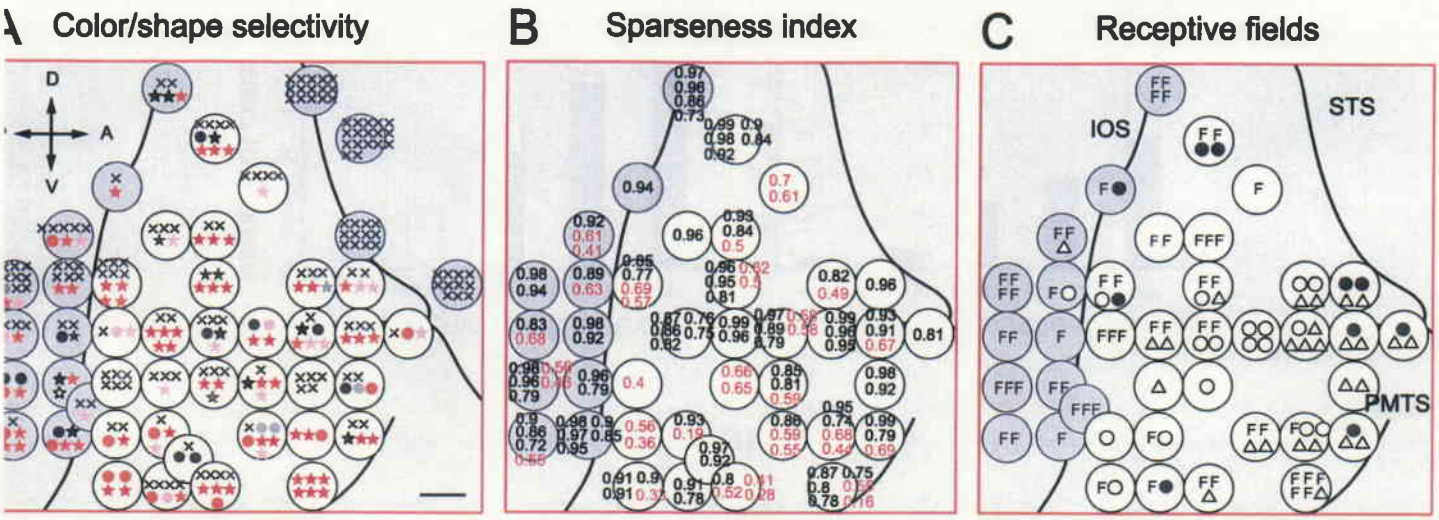
A
Color/shape selectivity
D
A
V
B
Sparseness index
C
Receptive fields
IOS
STS
PMTS

Fig. 12

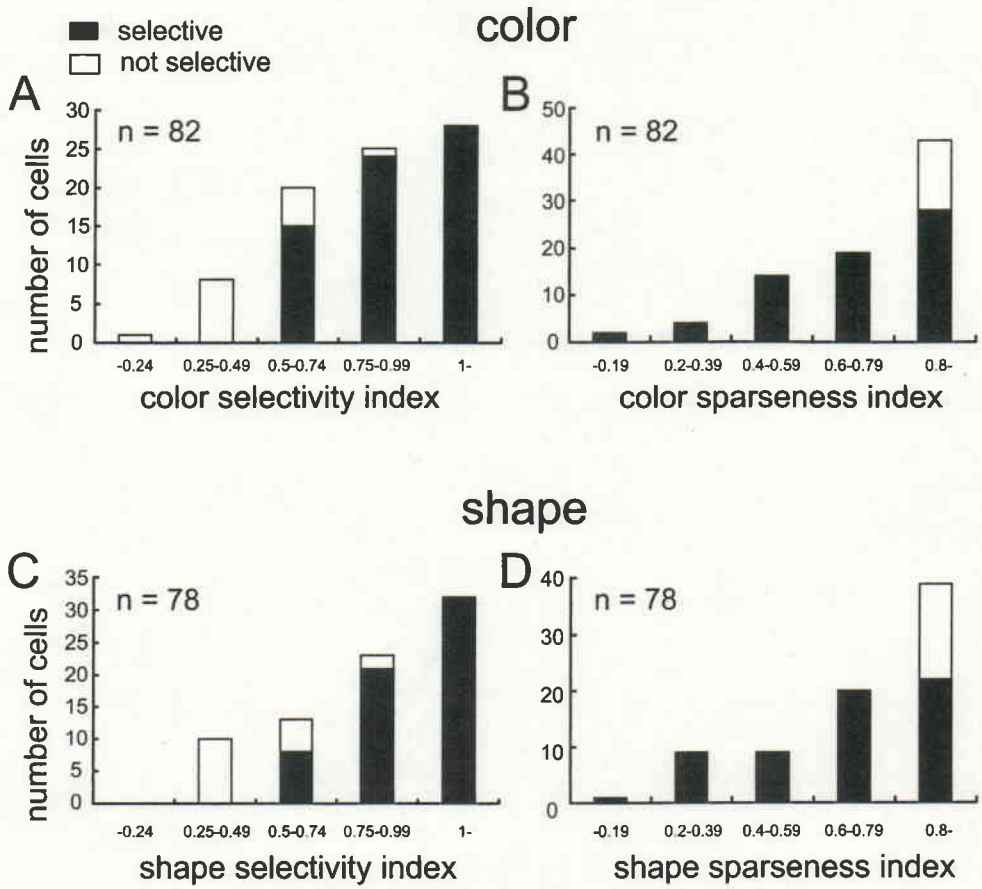
color
selective
not selective
A
B
n = 82
n = 82
number of cells
30
25
20
15
10
5
0
50
40
30
20
10
0
-0.24
0.25-0.49
0.5-0.74
0.75-0.99
1-
-0.19
0.2-0.39
0.4-0.59
0.6-0.79
0.8-
color selectivity index
color sparseness index
shape
C
D
n = 78
n = 78
number of cells
35
30
25
20
15
10
5
0
40
30
20
10
0
-0.24
0.25-0.49
0.5-0.74
0.75-0.99
1-
-0.19
0.2-0.39
0.4-0.59
0.6-0.79
0.8-
shape selectivity index
shape sparseness index

Fig. 13

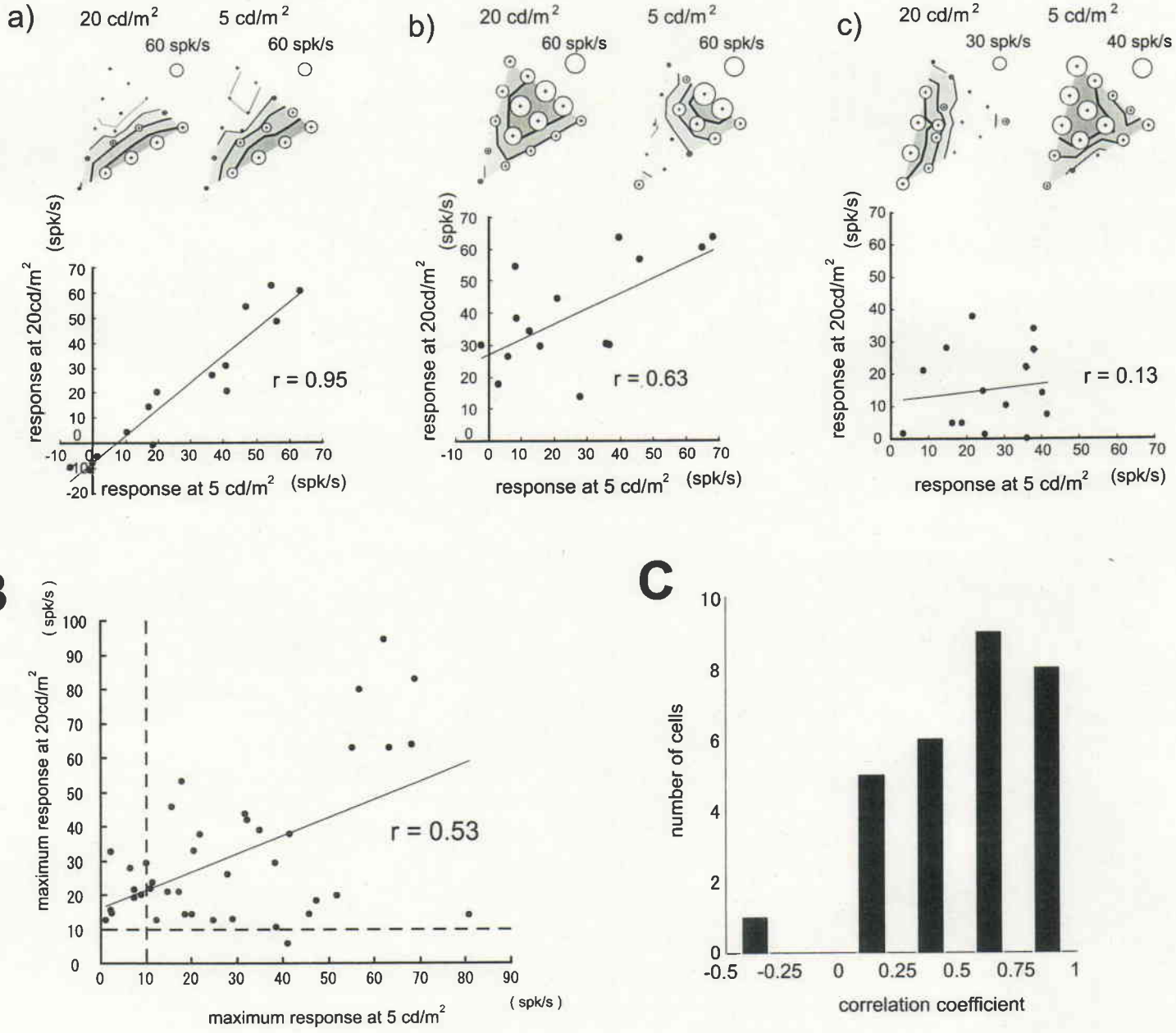
a)
20 cd/m2
5 cd/m2
60 spk/s
60 spk/s
response at 20cd/m2 (spk/s)
response at 5 cd/m2 (spk/s)
r = 0.95
b)
20 cd/m2
5 cd/m2
60 spk/s
60 spk/s
response at 20cd/m2 (spk/s)
response at 5 cd/m2 (spk/s)
r = 0.63
c)
20 cd/m2
5 cd/m2
30 spk/s
40 spk/s
response at 20cd/m2 (spk/s)
response at 5 cd/m2 (spk/s)
r = 0.13
B
maximum response at 20cd/m2 (spk/s)
maximum response at 5 cd/m2 (spk/s)
r = 0.53
C
number of cells
correlation coefficient

Fig. 14

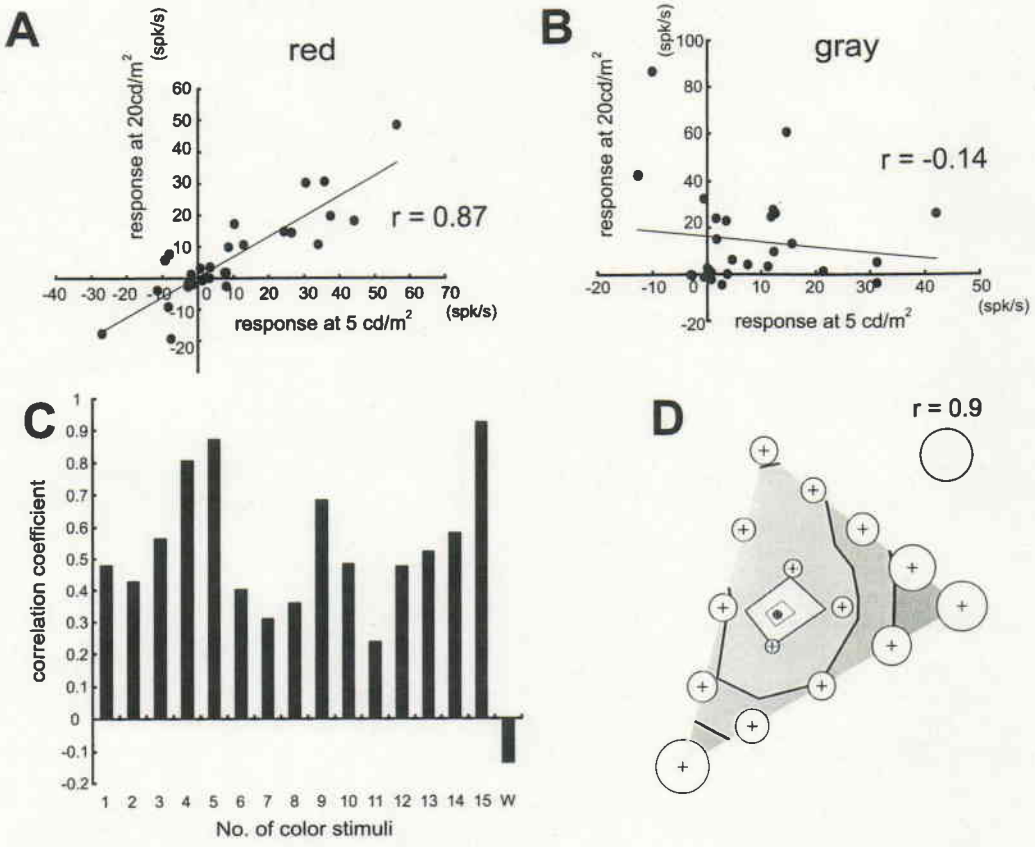
A
red
response at 20cd/m² (spk/s)
r = 0.87
response at 5 cd/m² (spk/s)
B
gray
response at 20cd/m² (spk/s)
r = -0.14
response at 5 cd/m² (spk/s)
C
correlation coefficient
No. of color stimuli
1 2 3 4 5 6 7 8 9 10 11 12 13 14 15 W
D
r = 0.9

Fig. 15